Heating, Confinement, and Stirring in the Madison Plasma Dynamo Experiment

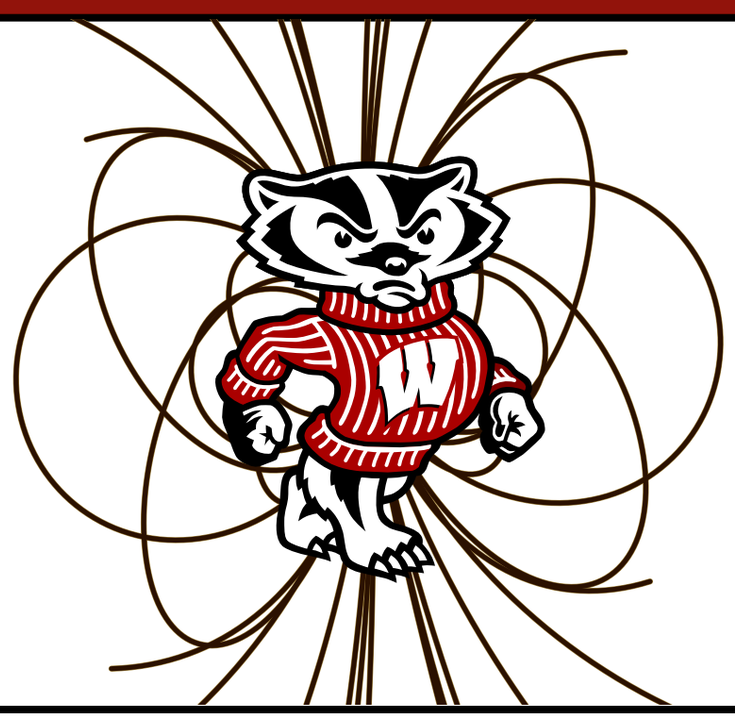

Cary Forest

M. Clark, C. Cooper, K. Flanagan,
I. Khalzov, Y. Li., J. Milhone,
E. Peterson, M. Wallace, D. Weisberg,
and the MPDX team

NSF

CMSO

Dynamo Experiments Require:

Frozen in flux: $Rm = \mu_0 \sigma UL \gg 1$

Flow Dominated: $\rho U^2 \gg B^2/\mu_0$

New regime for plasma experiments–
astrophysical applications

Hydrodynamics: Re = UL/, Pm=Rm/Re

Pursuing a laboratory dynamo

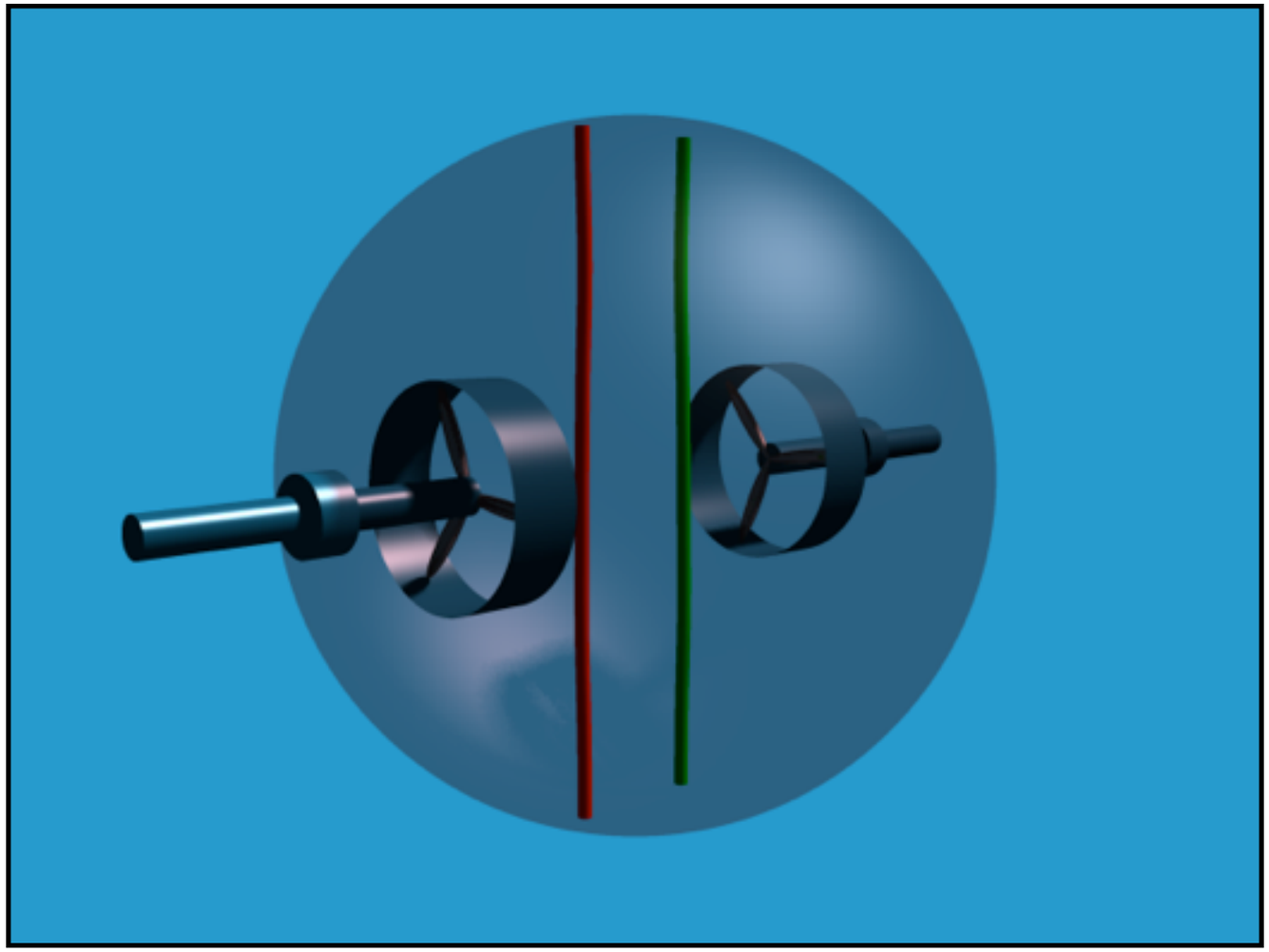

Plasmas are Challenging

-difficult to stir

-some confinement required with weak B

Use Liquid Metals

-confinement is free

-easy to stir

-BUT power scaling is challenging: $P_{mech} \sim Rm^3 / L$

[Rm=100, P_{mech}=100 kW]

-Re = 10^7 (Pm=10^{-5}, turbulent)

Liquid metal Dynamos Experiments: Low Rm, high Re

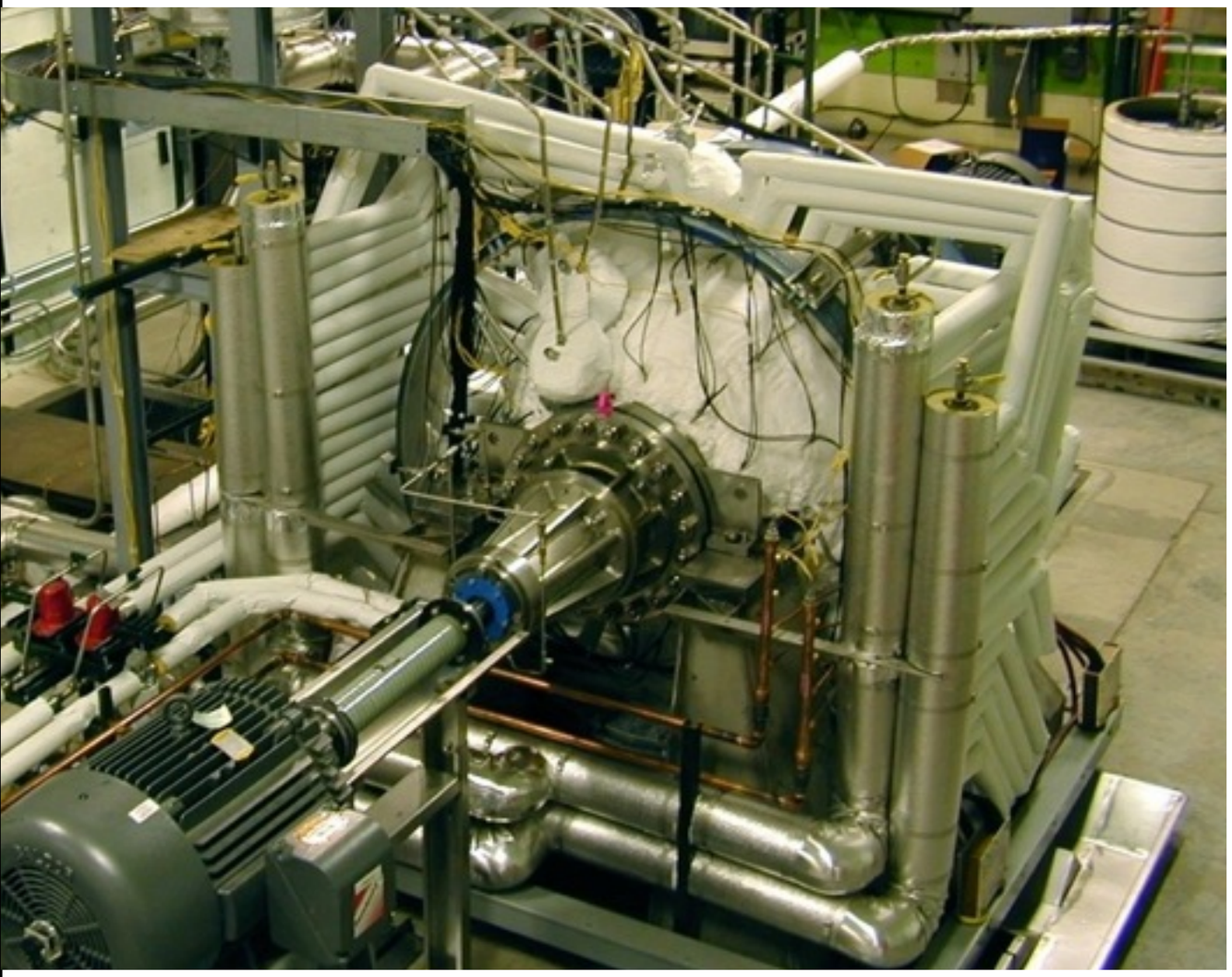

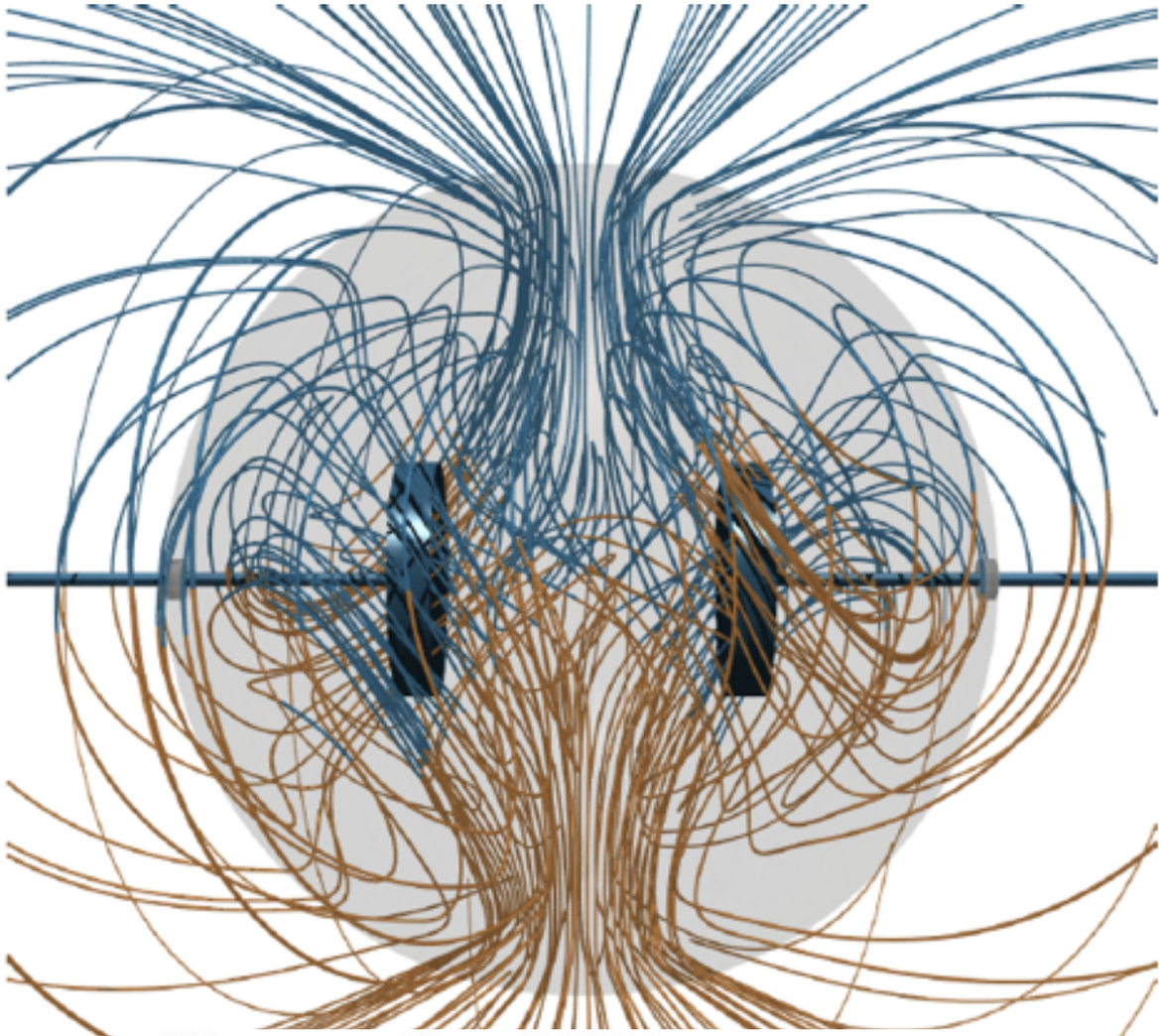

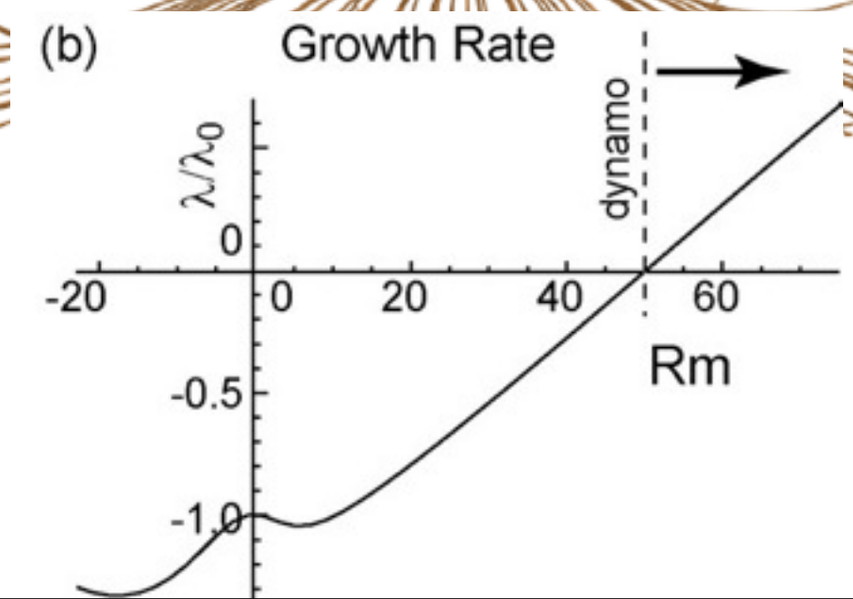

The Madison Dynamo Experiment
a=0.5m, V=10 m/s
P=150kW, Rm_{max}=100

Unconstrained Liquid metal experiments are dominated by turbulence (resistivity), which governs dynamo onset

For liquid metals Re~10^5 Rm

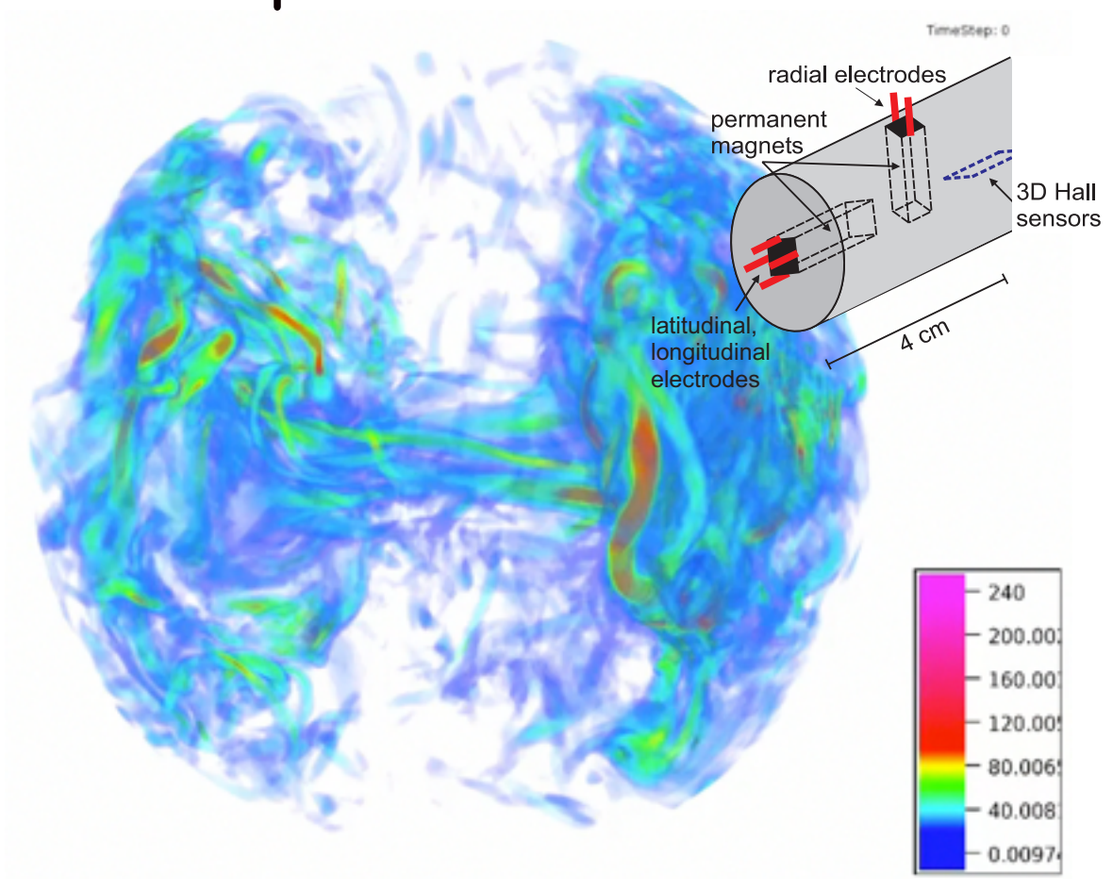

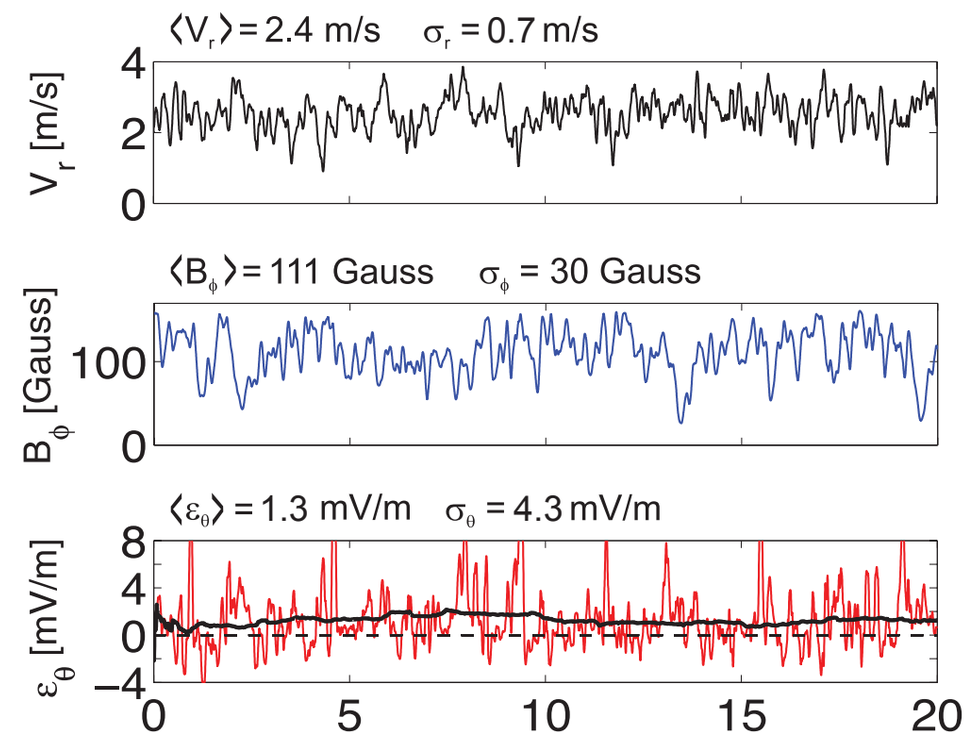

$$\varepsilon^{turb} = \left\langle \tilde{\mathrm{v}} \times \tilde{\mathrm{b}} \right\rangle_{\phi}$$

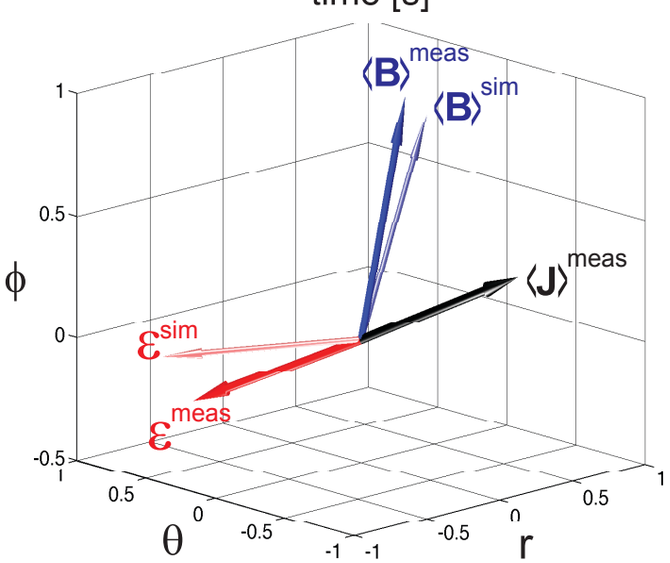

Direct Observation of a Turbulent EMF and transport of a magnetic field in a liquid sodium dynamo experiment, The Astrophysical Journal, **759** 80 2012.

$$\eta_{eff} = \eta + \frac{\tilde{v}\ell}{3}$$

Two-vortex flow driven by controlling rotation on plasma boundary

Modified Von Karman flow

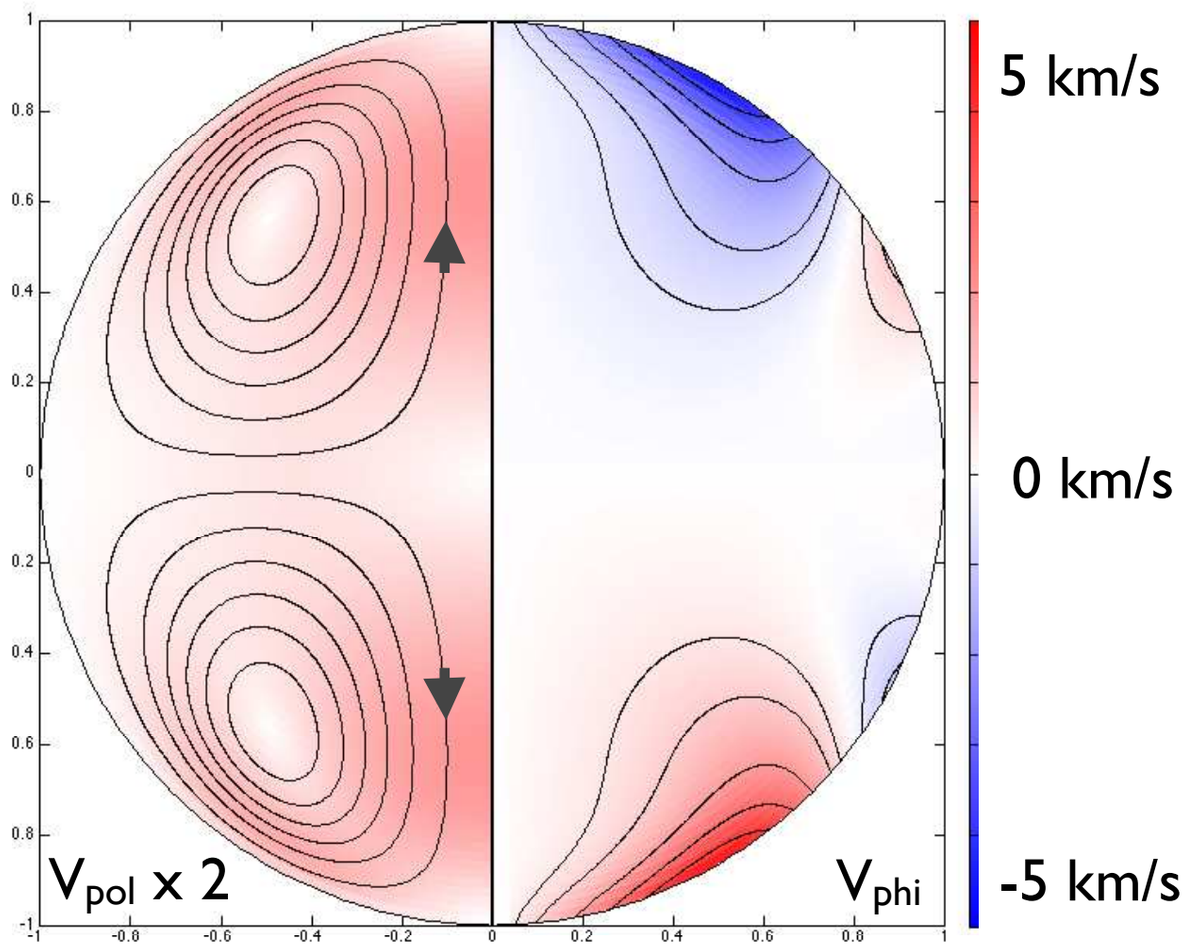

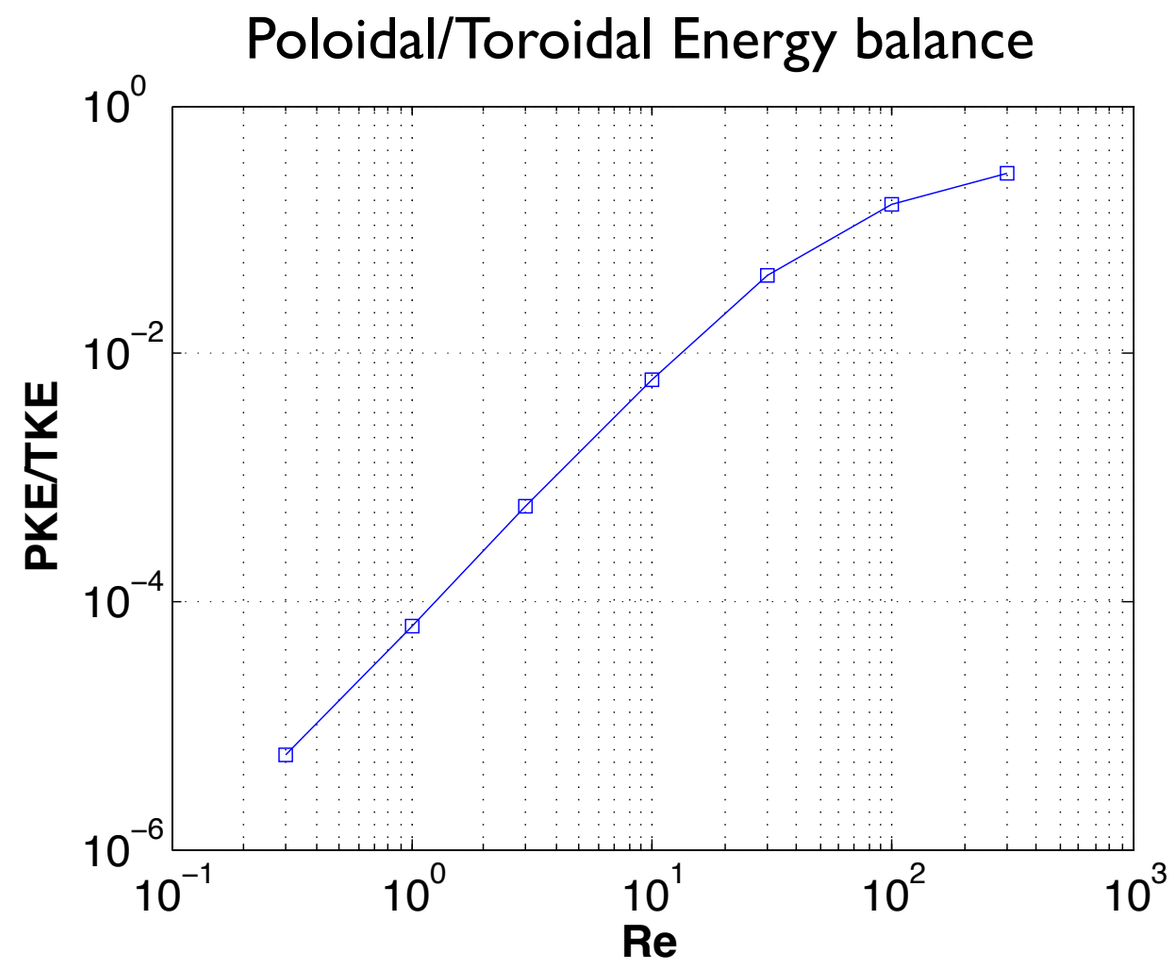

Re=100

pure hydro solution to Navier Stokes

Poloidal forcing is larger for inviscid plasmas

Generating two-vortex flow in a plasma

Dynamo experiments require:

$\mathrm{Re} = UL/\eta = 7.8\frac{n_{18}\sqrt{\mu}Z^4U_{km/s}L_m}{T_{i,eV}^{5/2}}$	**>100**	Dense
$\mathrm{Rm} = \mu_0\sigma UL = 1.6\frac{T_{e,eV}^{3/2}U_{km/s}L_m}{Z}$	**>>1**	Hot
$M_A = \sqrt{\mu_0\rho}U/B = 0.46\frac{\sqrt{n_{18}\mu}U_{km/s}}{B_G}$	**>>1**	Unmagnetized
		Flowing

Flowing, unmagnetized plasmas in the Lab

Plasma Couette Experiment

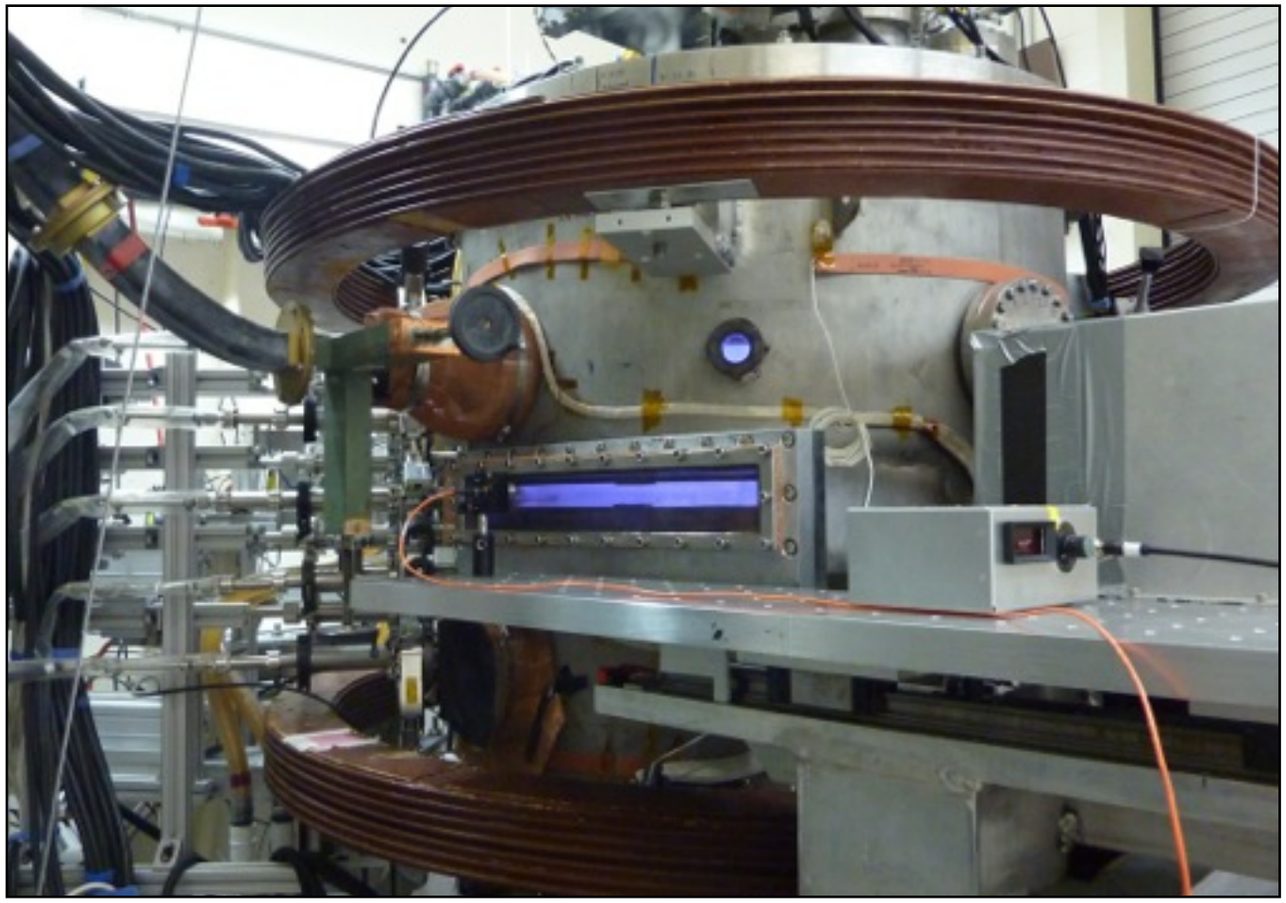

Madison Plasma Dynamo Experiment

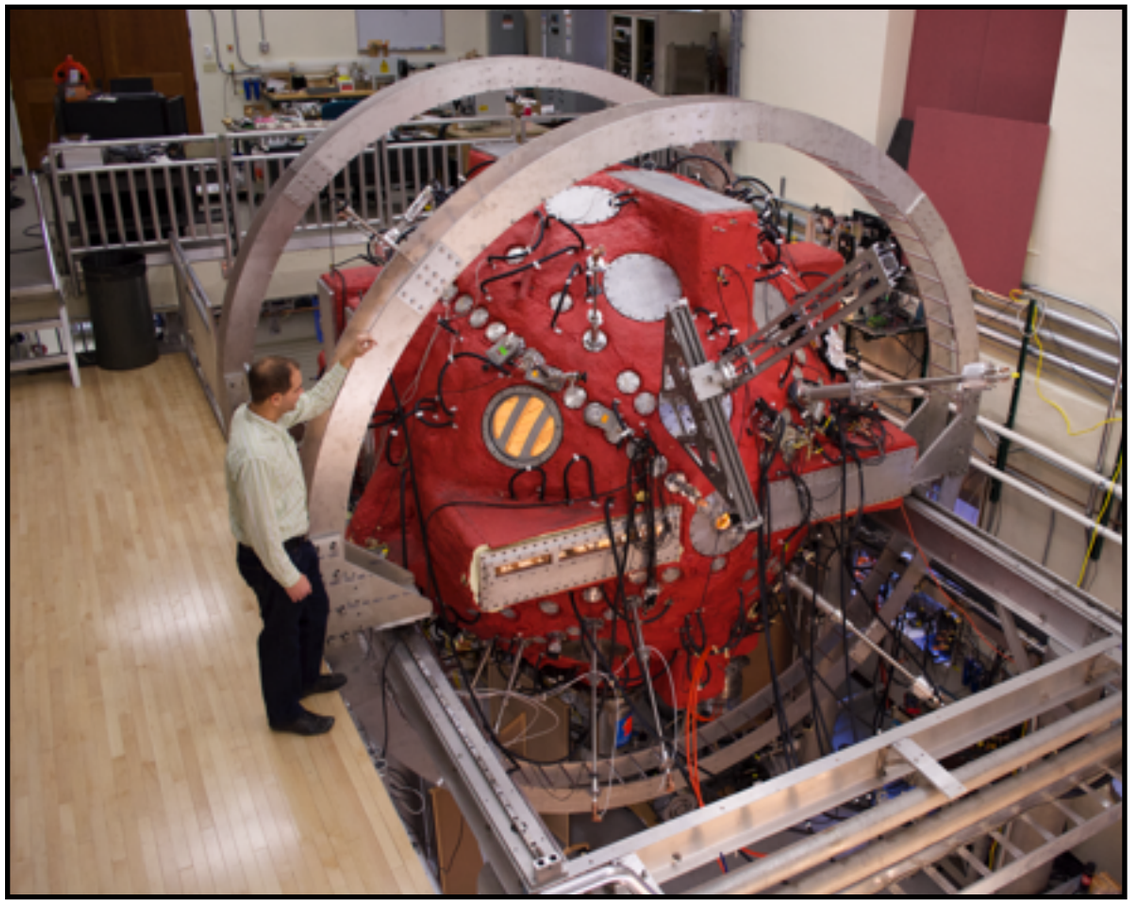

MPDX plasmas exceed critical Rm for dynamo

Achieved parameters

Te	20 eV
ne	1 x 10
V	6.0 km/s

Re = 200

Rm = 350

Dynamo onset vs. Re

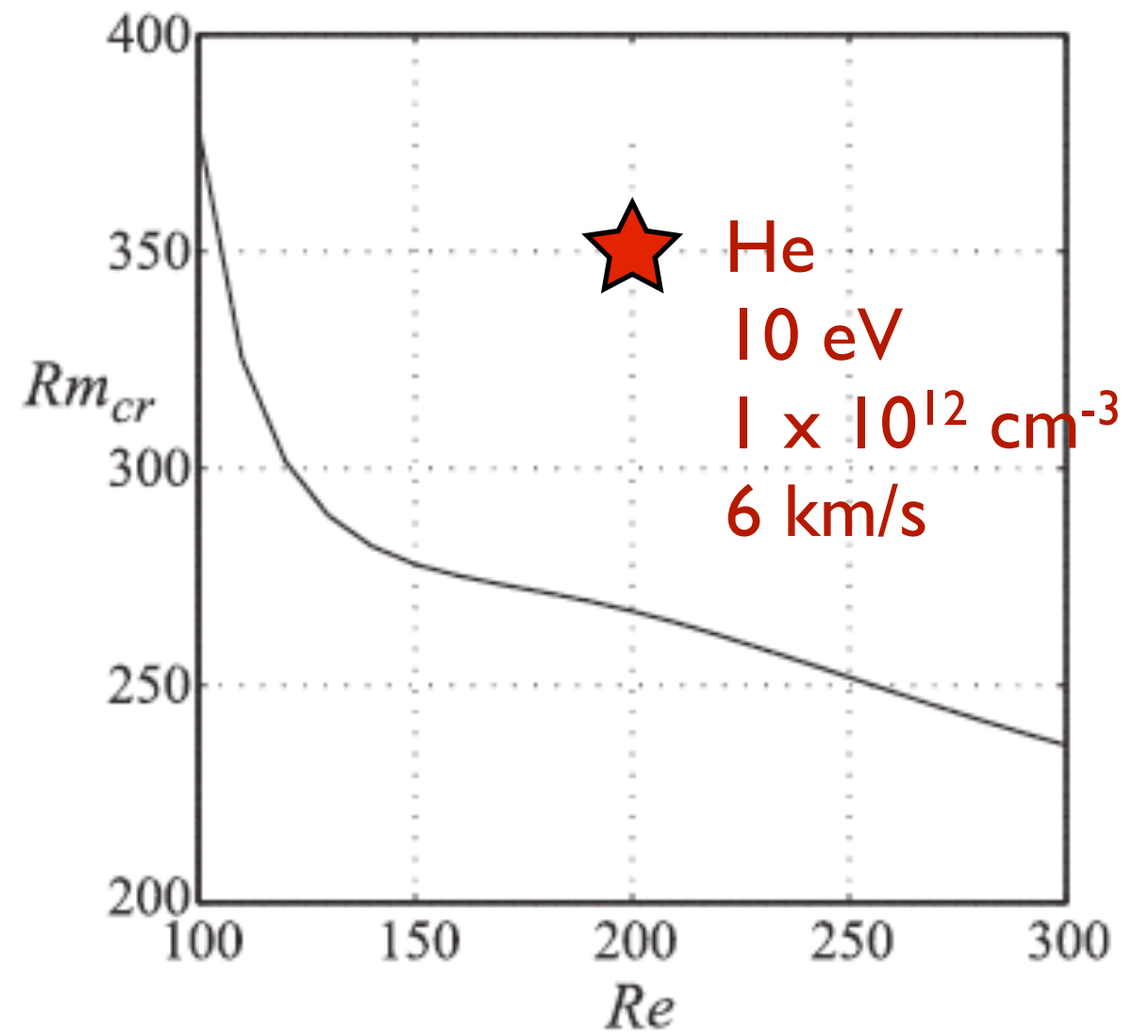

Khalvov, et al, *Optimized boundary driven flows for dynamos in a sphere,* Phys. Plasmas **19** 112106 (2012).

The Madison Plasma Dynamo Experiment

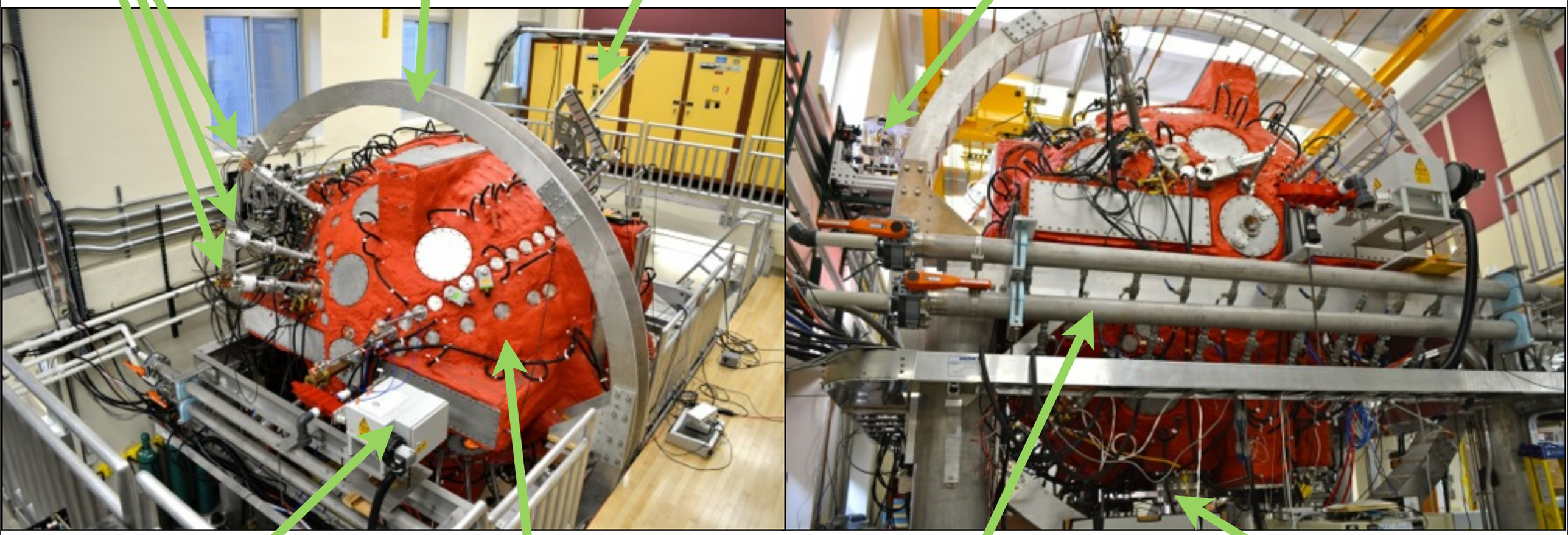

confinement: Permanent magnets in ring cusp geometry

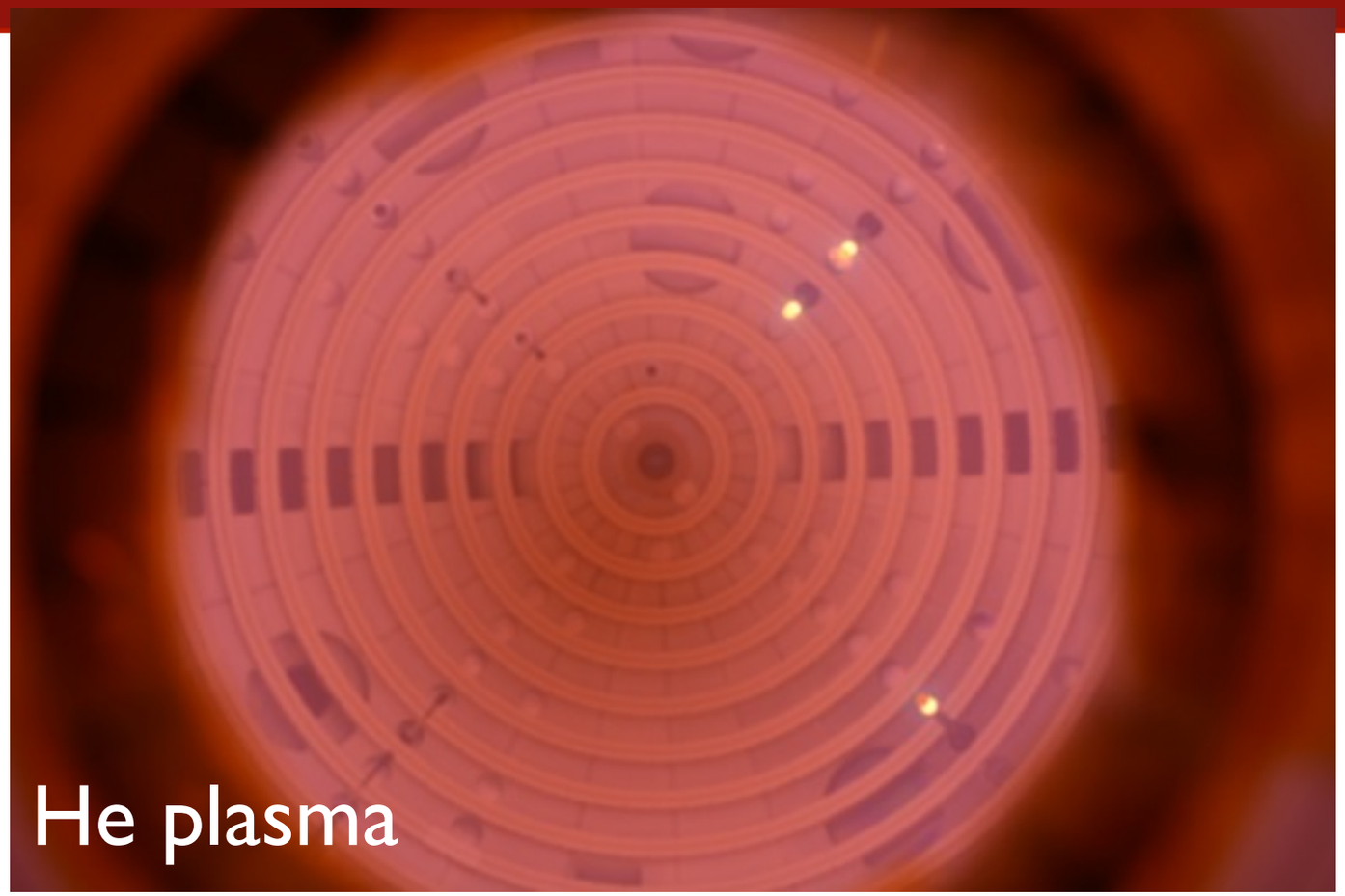

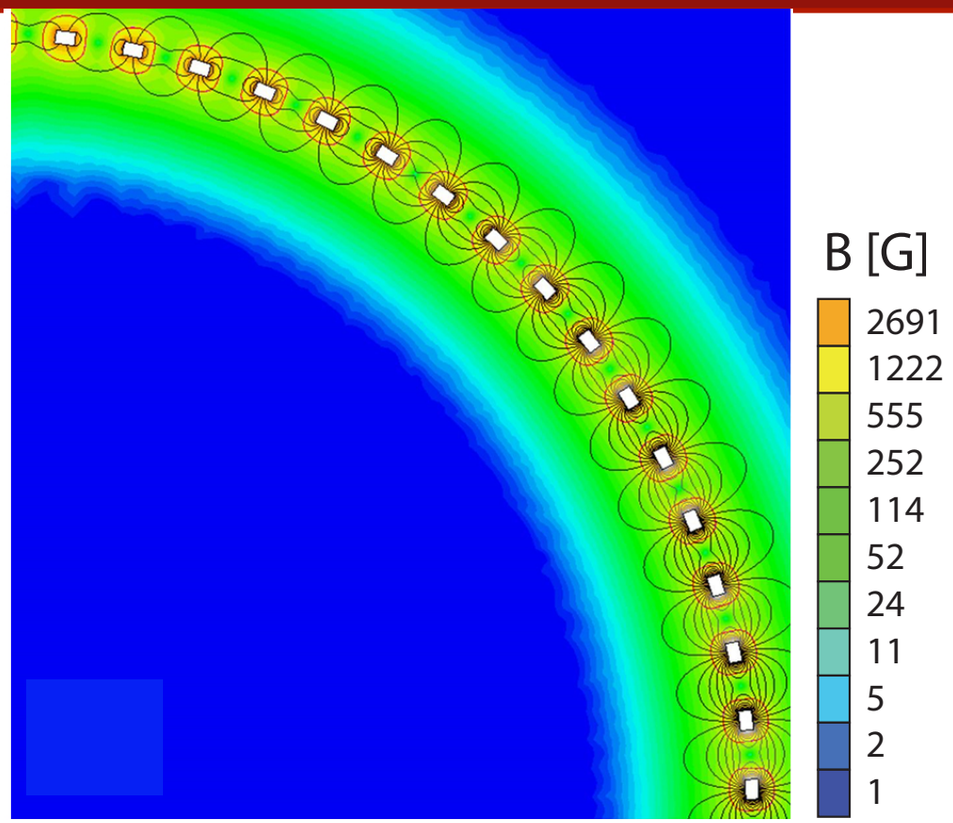

Cusp field cross-section

Cusp loss width: $w_c \approx 4\sqrt{\rho_e \rho_i} = 0.08 \text{ cm}$

Particle Balance:

$$\iiint \langle \sigma_{iz} v_e \rangle n_e n_n \mathrm{d}V = 0.5 n_e c_s (A_c + A_l)$$

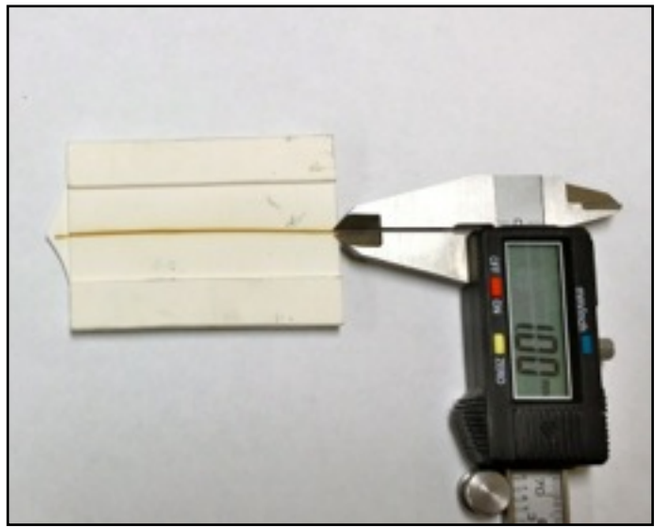

Ceramic limiter tiles show cusp width

3000 4 kG SmCo magnets

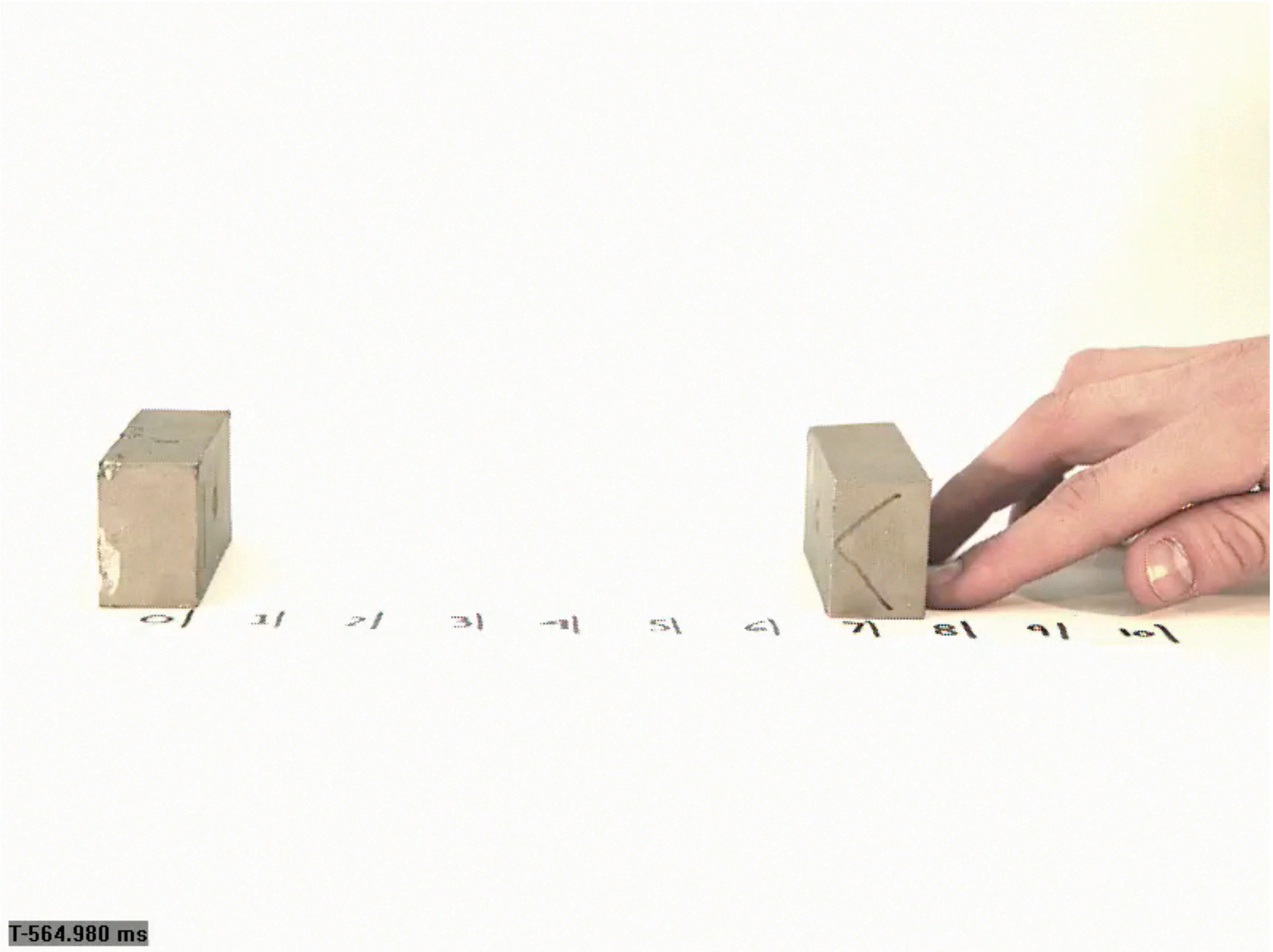
T-564.980 ms

Plasma Heating an Stirring: LaB_6 cathodes

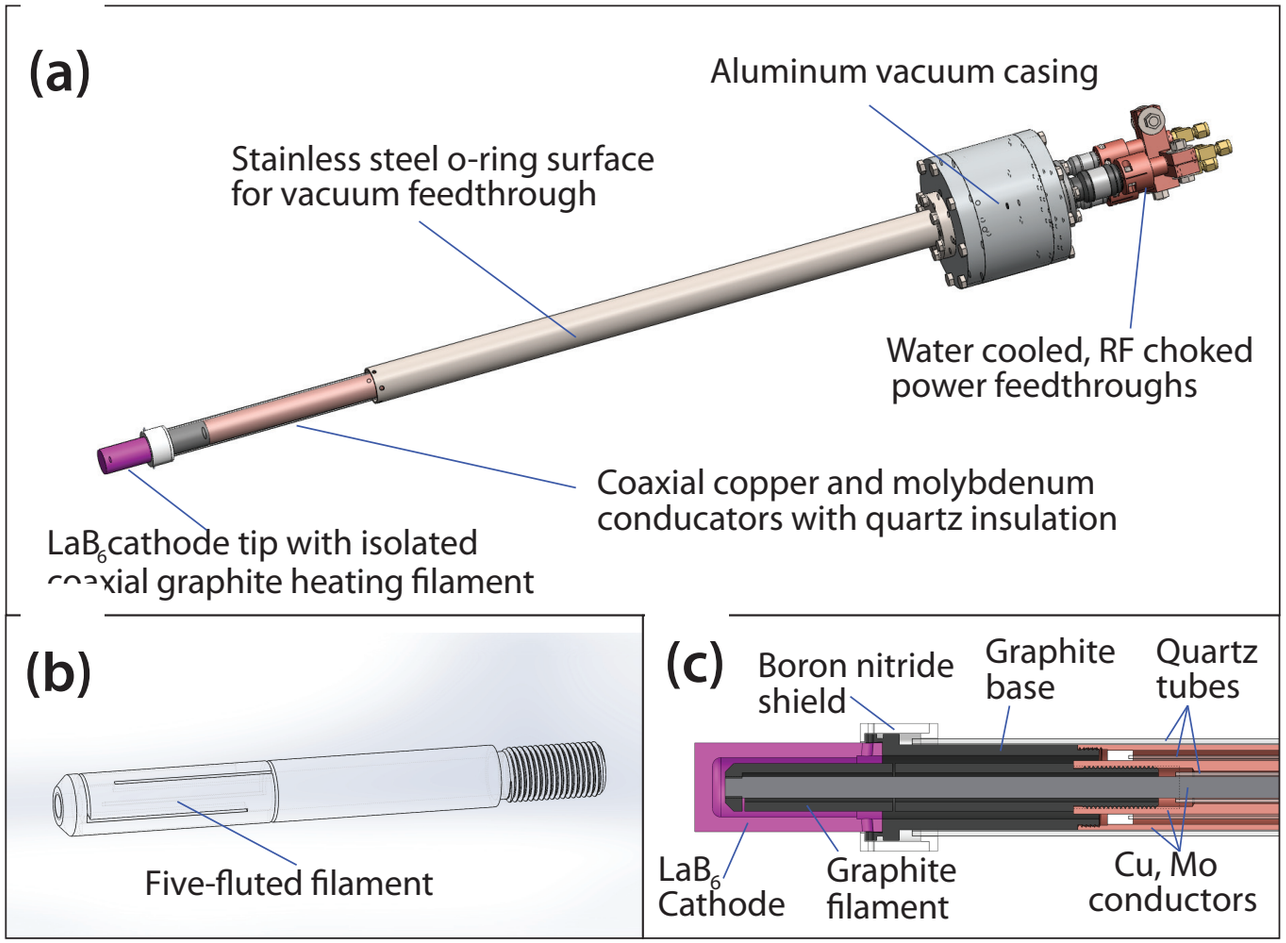

Discharge Voltage	Discharge Current	Discharge Power	Uptime
200-500 V	< 80 A	< 35 kW	> 4 months

Total installed power: 200kW

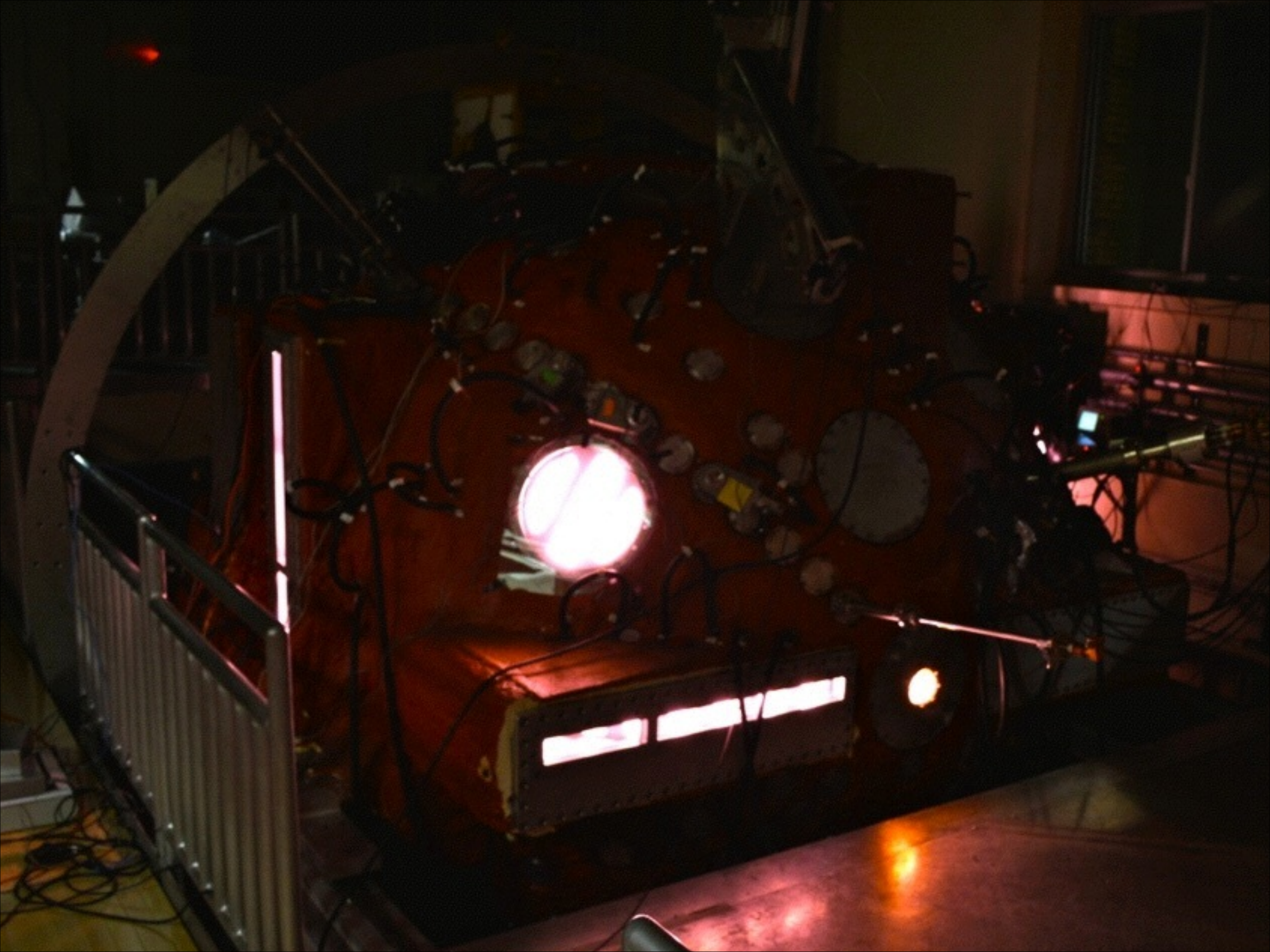

Hot, dense, high fractional ionization plasmas

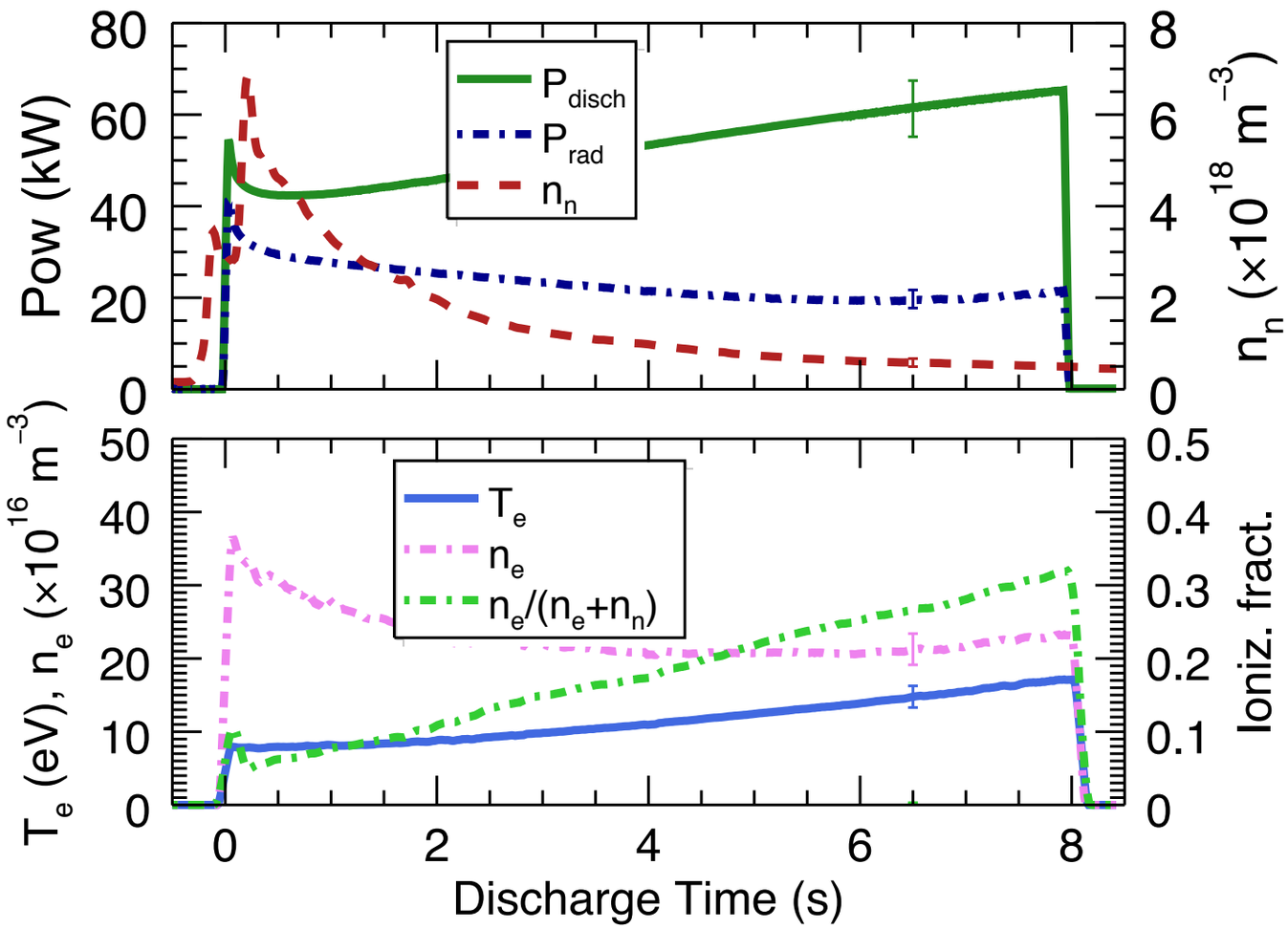

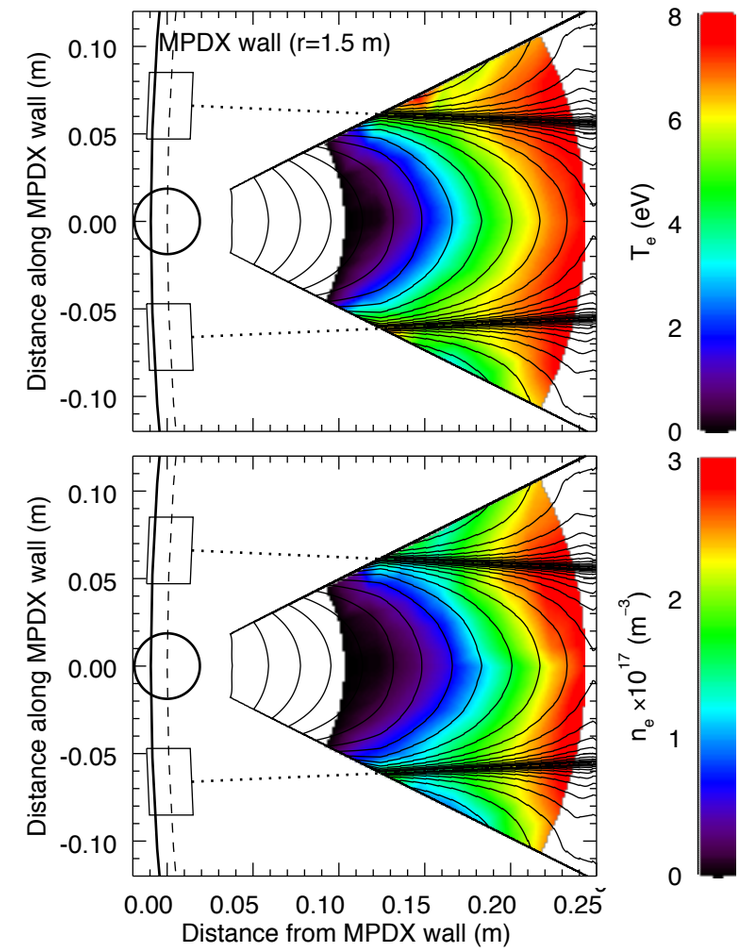

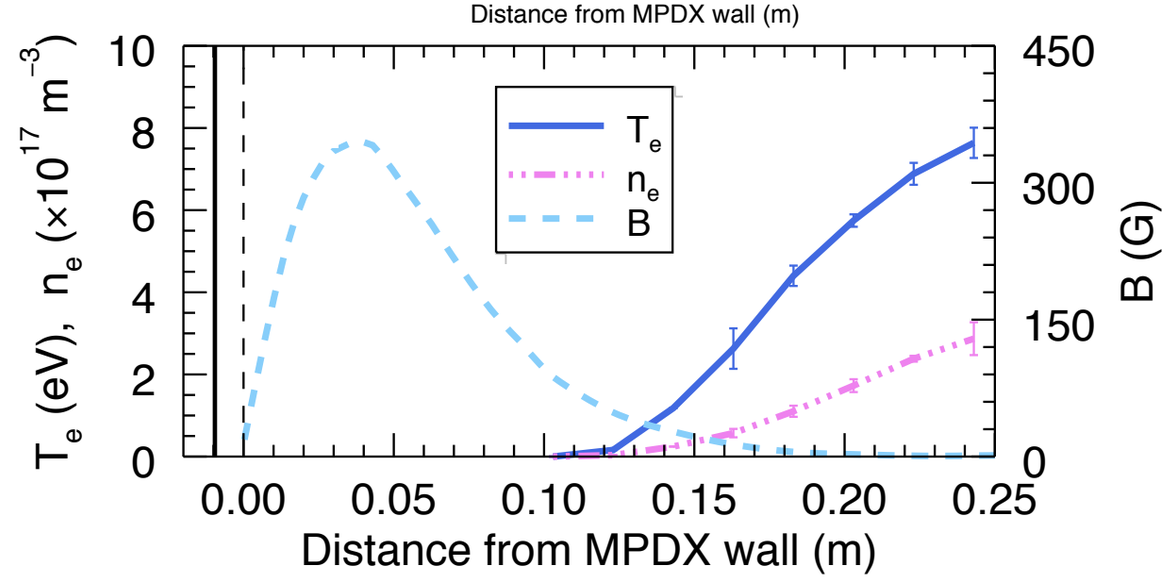

Cooper et al *The Madison plasma dynamo experiment: A facility for studying laboratory plasma astrophysics,* Phys. Plasmas **21** 013505 (2013).

VPIC results and measurements

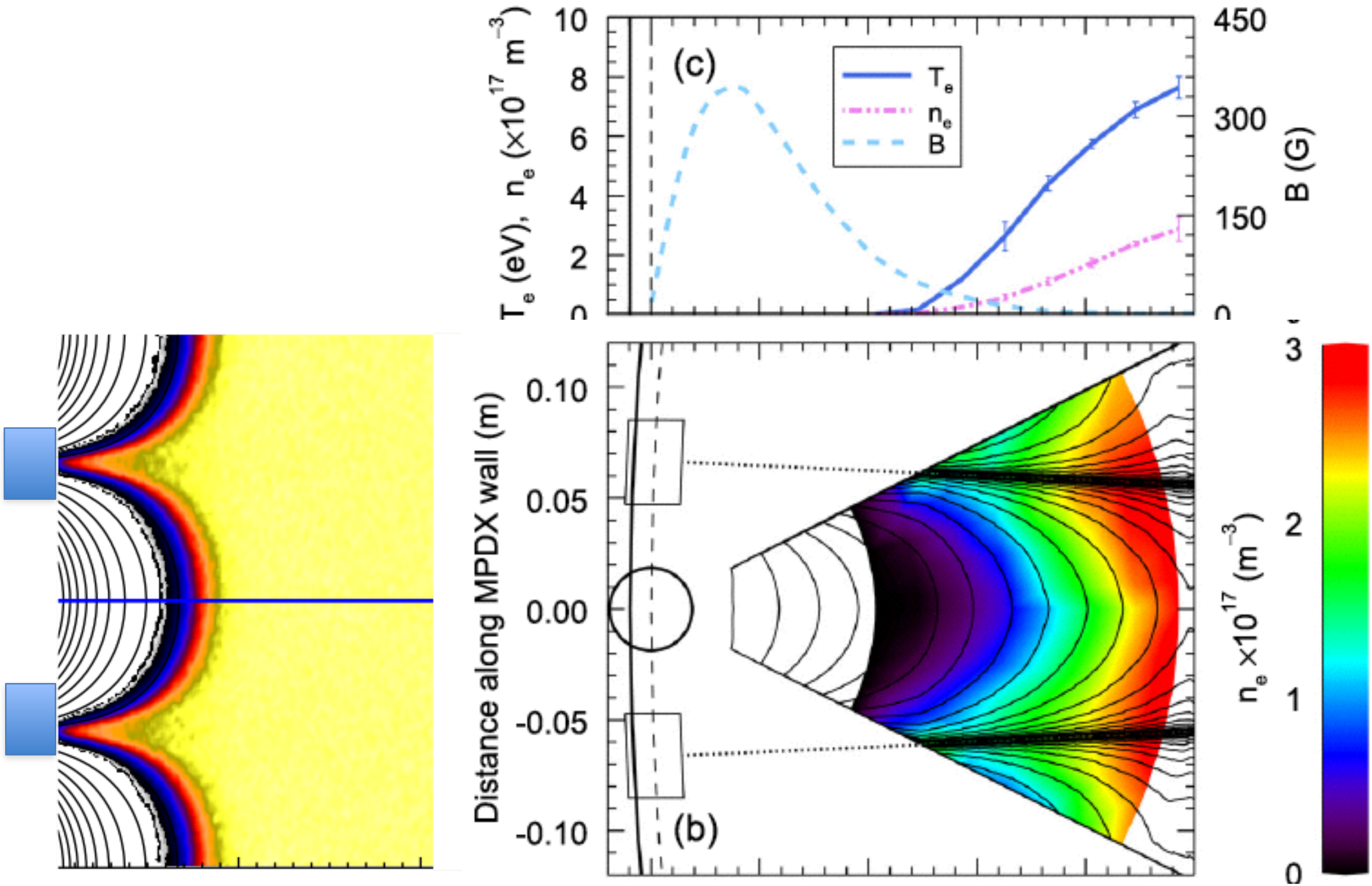

Cathode stirring experiments

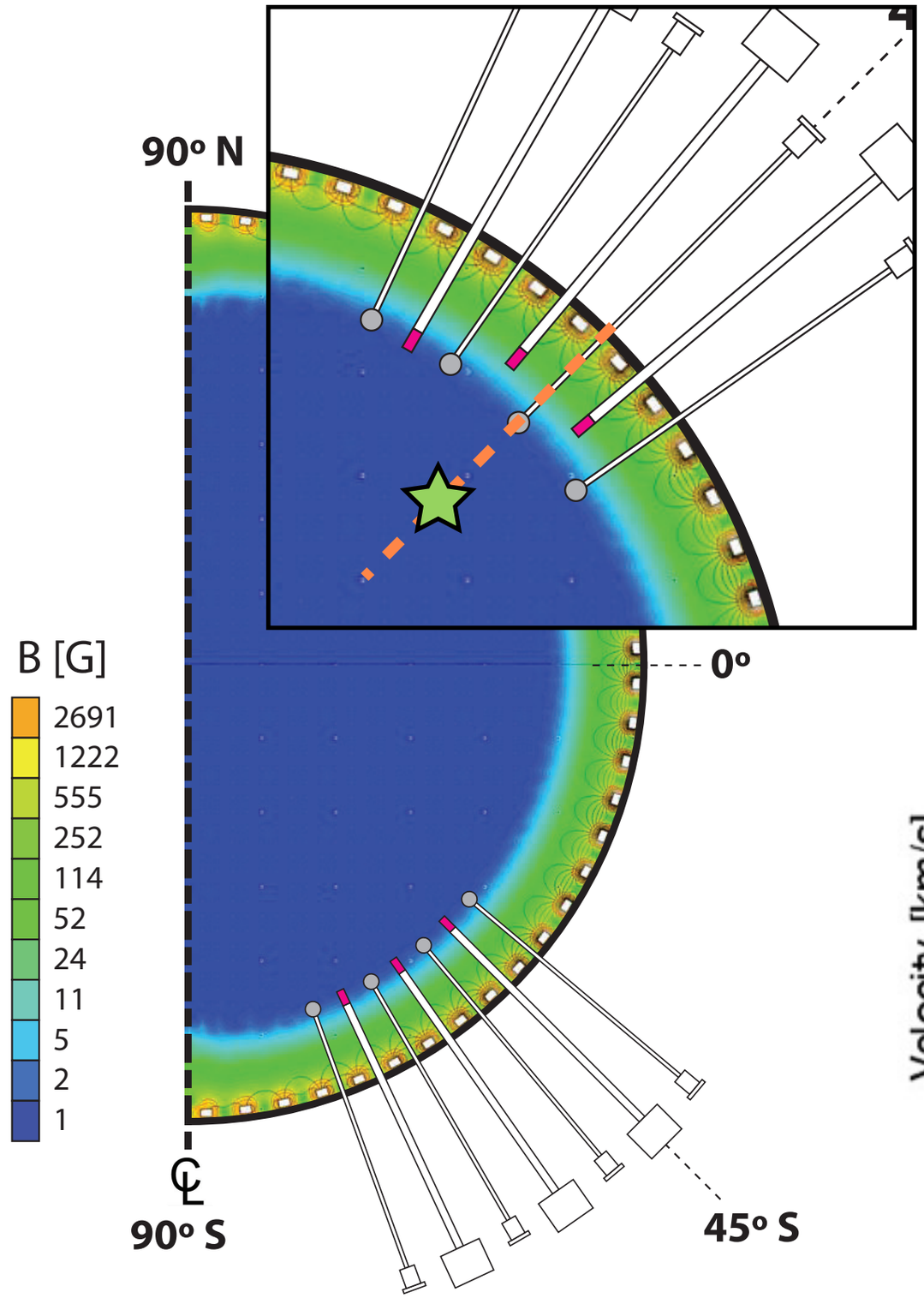

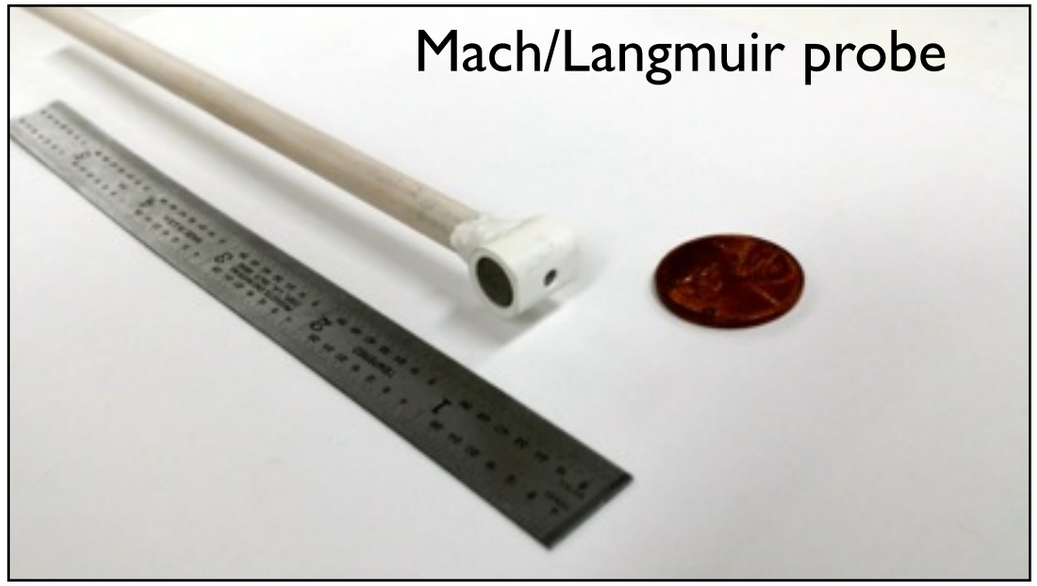

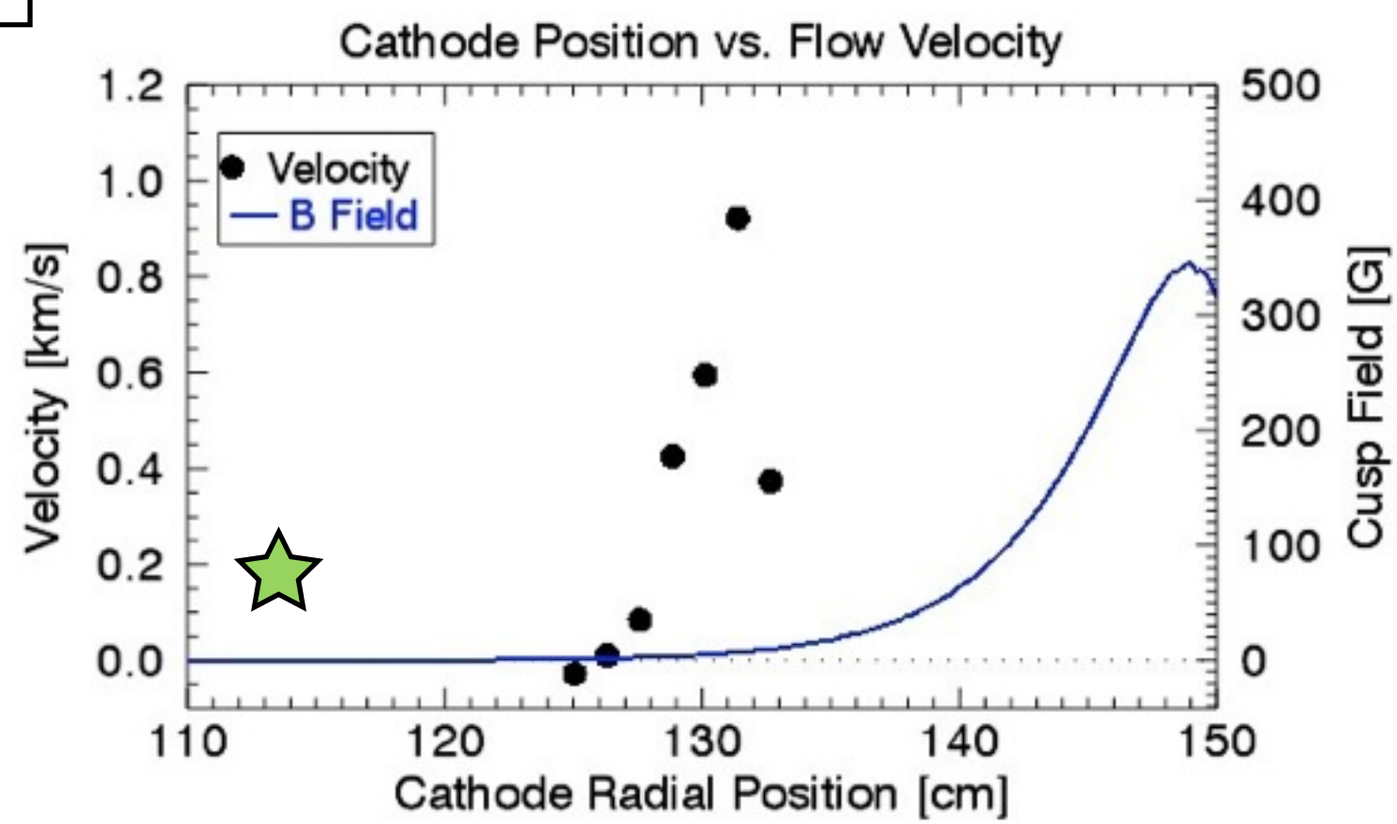

2-Cathode Stirring Measurements

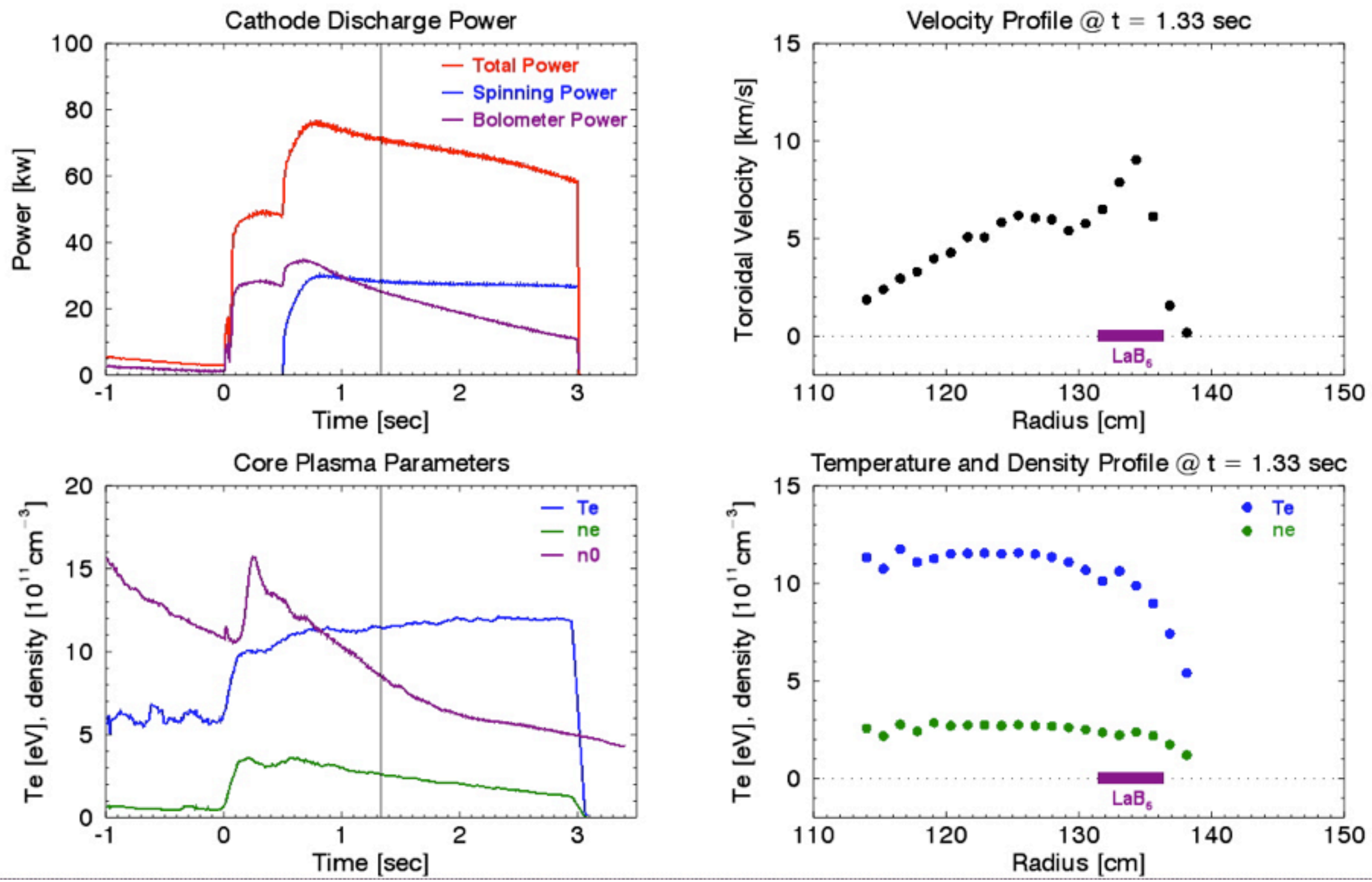

Hydromodeling will guide flow optimization

2 cathode flow

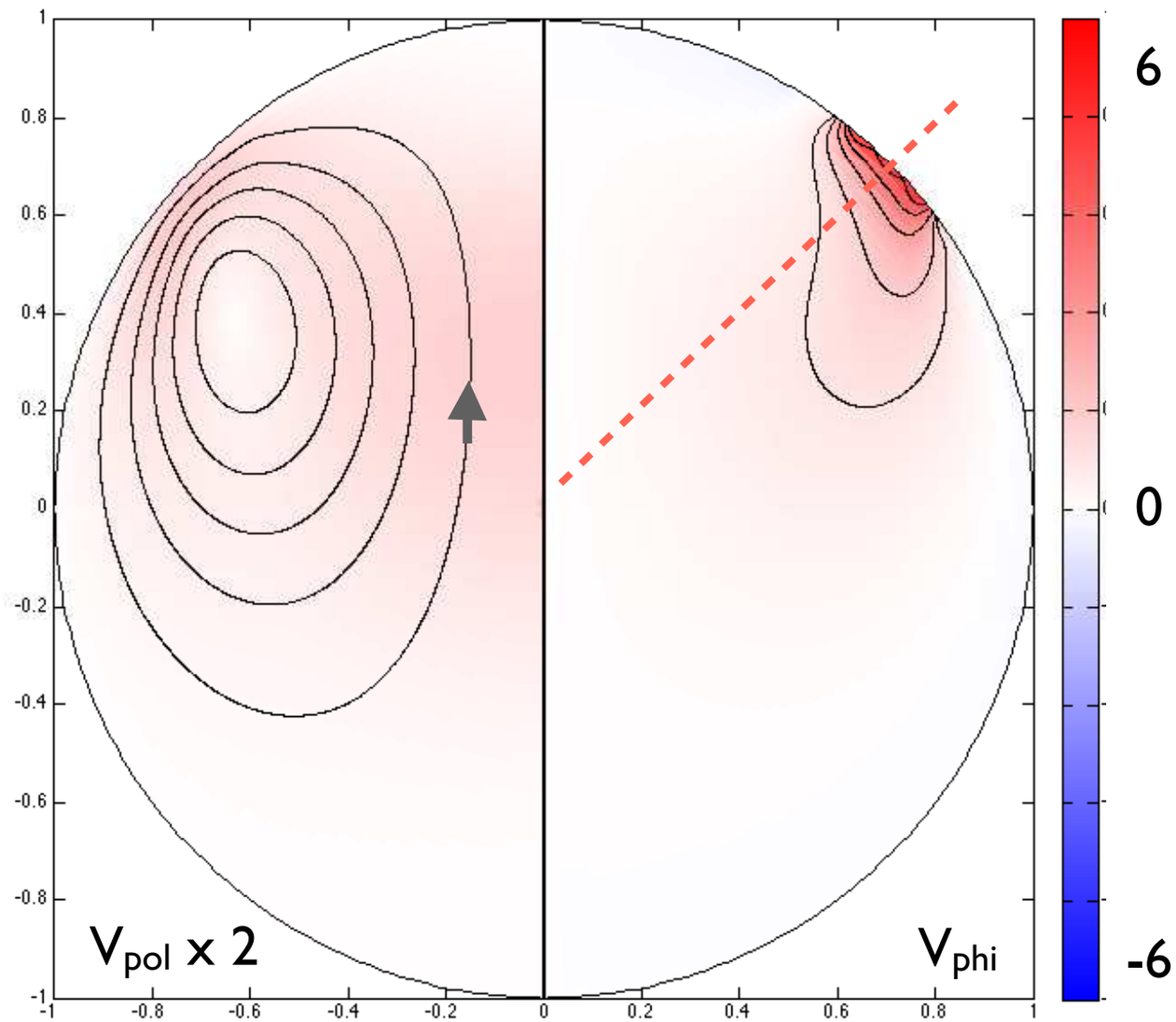

Re = 200

Velocity data shows expected momentum coupling

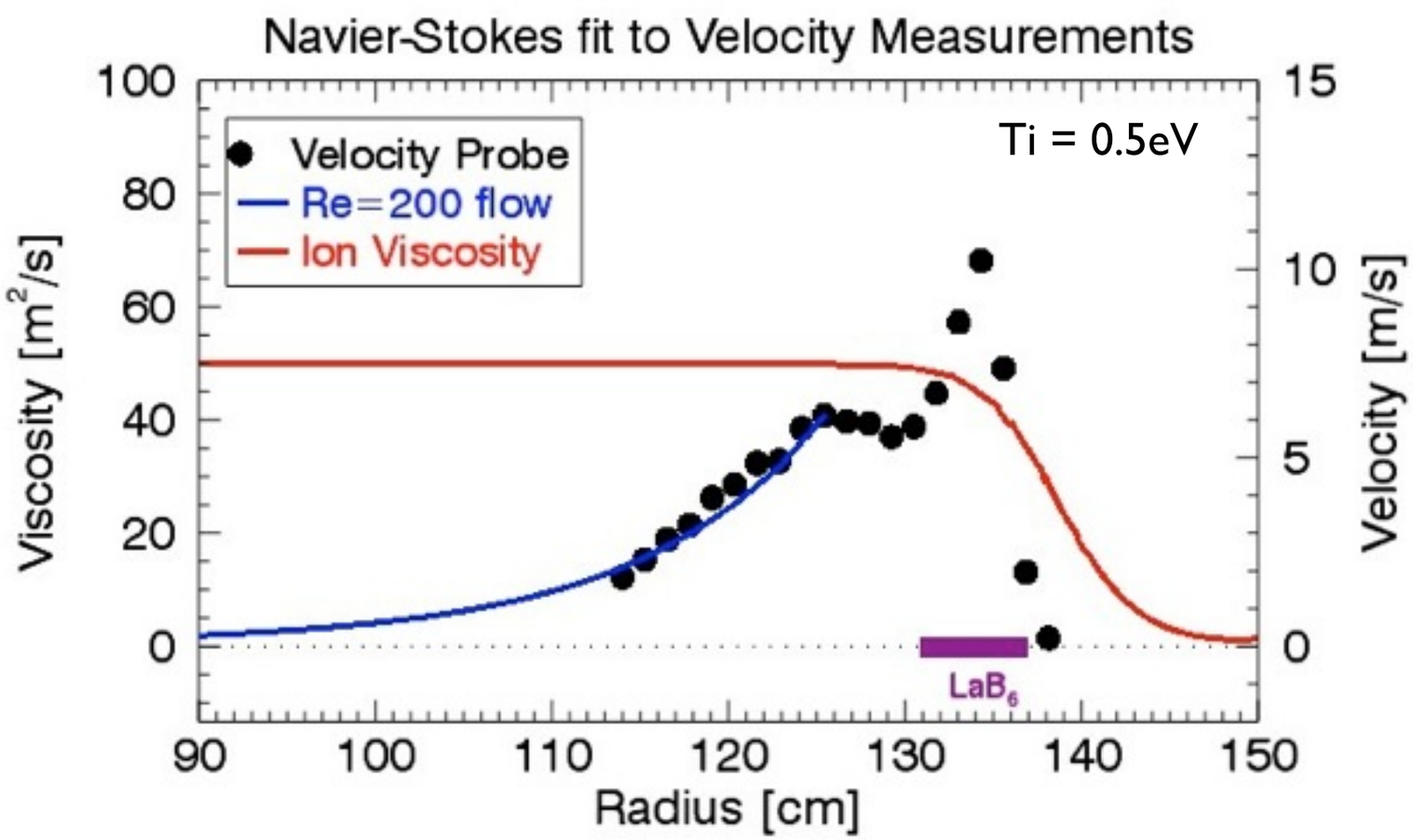

2 cathode flow

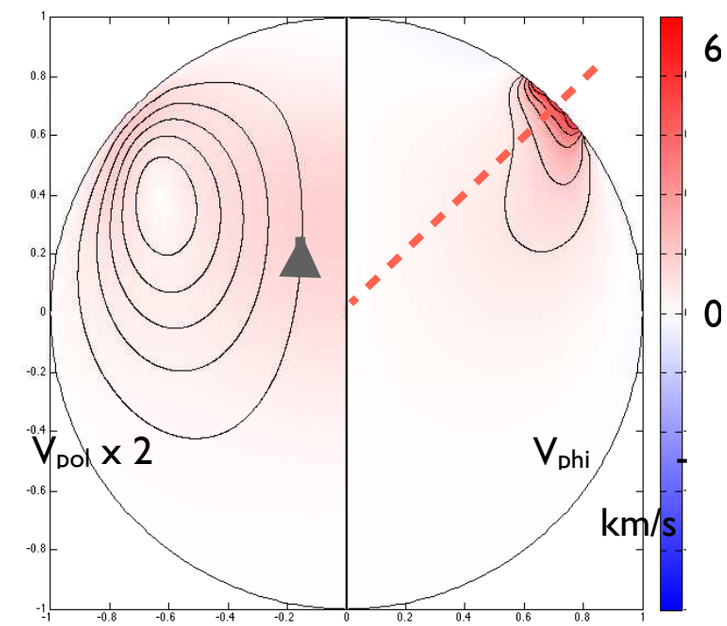

Re = 200

$$\nu_0^i = 0.96\tau_{ii}v_{ti}^2 \sim \frac{T_i^{5/2}}{n_i\sqrt{\mu}}$$

$$\nu_{mag}^i = \frac{3}{10}\frac{\rho_i^2}{\tau_{ii}} \sim \frac{n_i\sqrt{\mu}}{B^2\sqrt{T_i}}$$

- Stirring profile extends into unmagnetized core where ion viscosity is constant.

Next Step: 12 cathodes to search for a dynamo transition

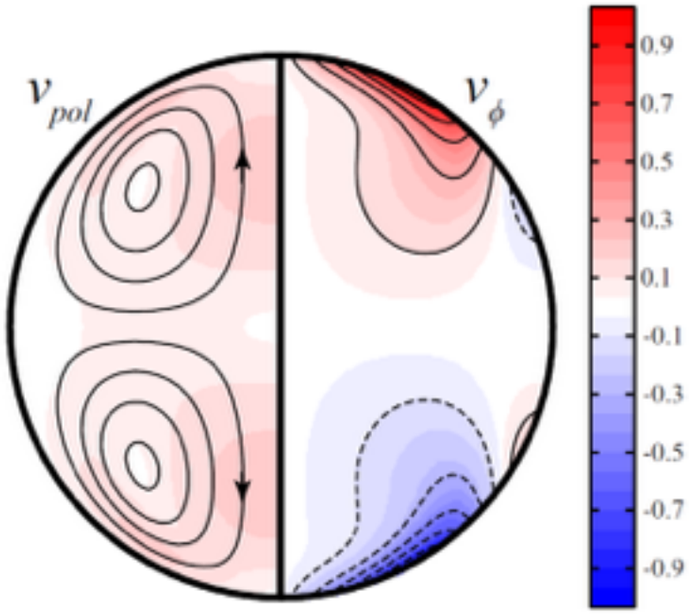

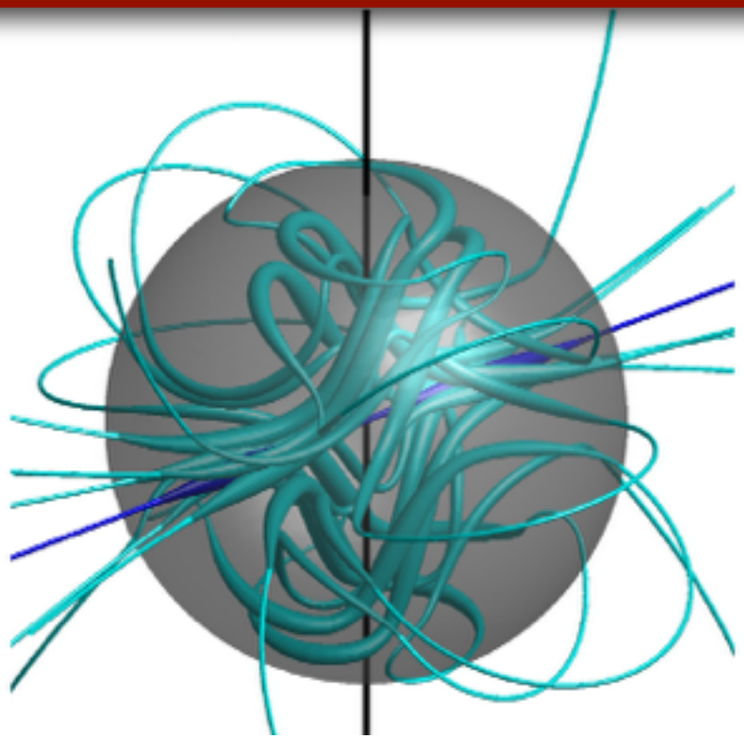

Dynamo growth rate

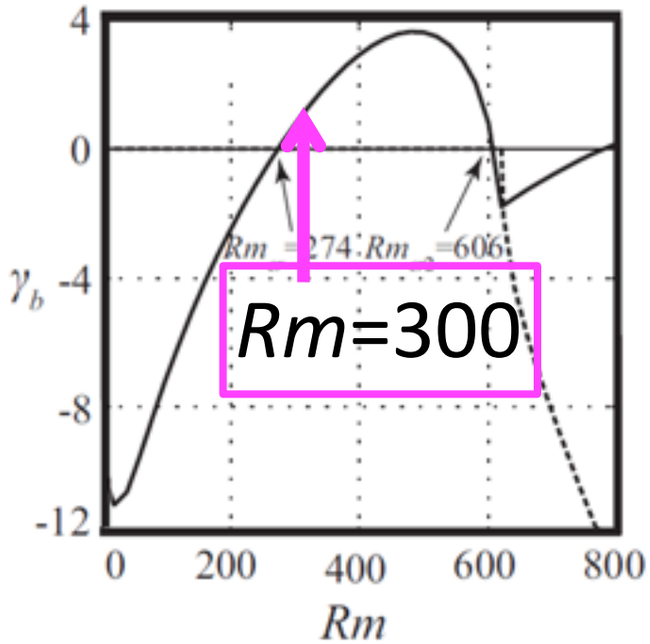

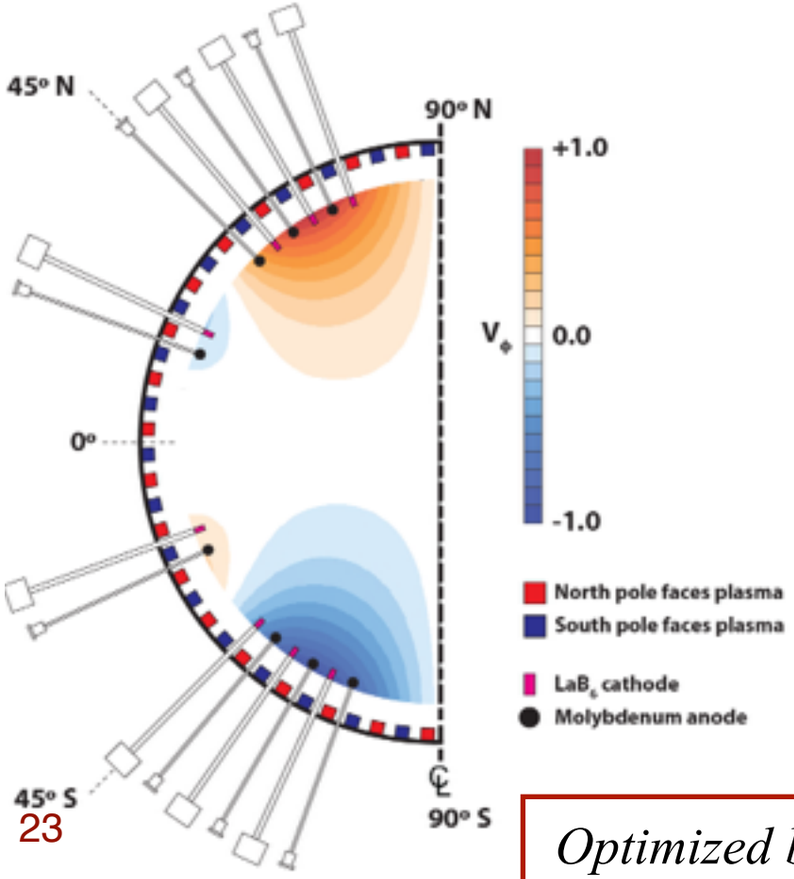

Von Karman type dynamo		
Re=150, Rm=400		
Parameter	Argon	Helium
n	3X10	1X10
T	10	10
power (kW)	100	140
v	5	6
B	8	5

Steady state flows with DC LaB_6 bias set $v_\phi(\theta)$

Optimized boundary driven flows for dynamos in a sphere, Phys. Plasmas **19** 112106 (2012).

Other Facility Possibilities

1. Fast Dynamos and Turbulence
2. Helioseismology
3. Kinetic, low collisionality physics
4. Reconnection (more from Egedal)
5. Alfven Waves a high Beta
6. Pulsar and Stellar Winds

Heating and confinement modeled by power/ particle balance

Confinement scaling law benchmarked by extensive power scan

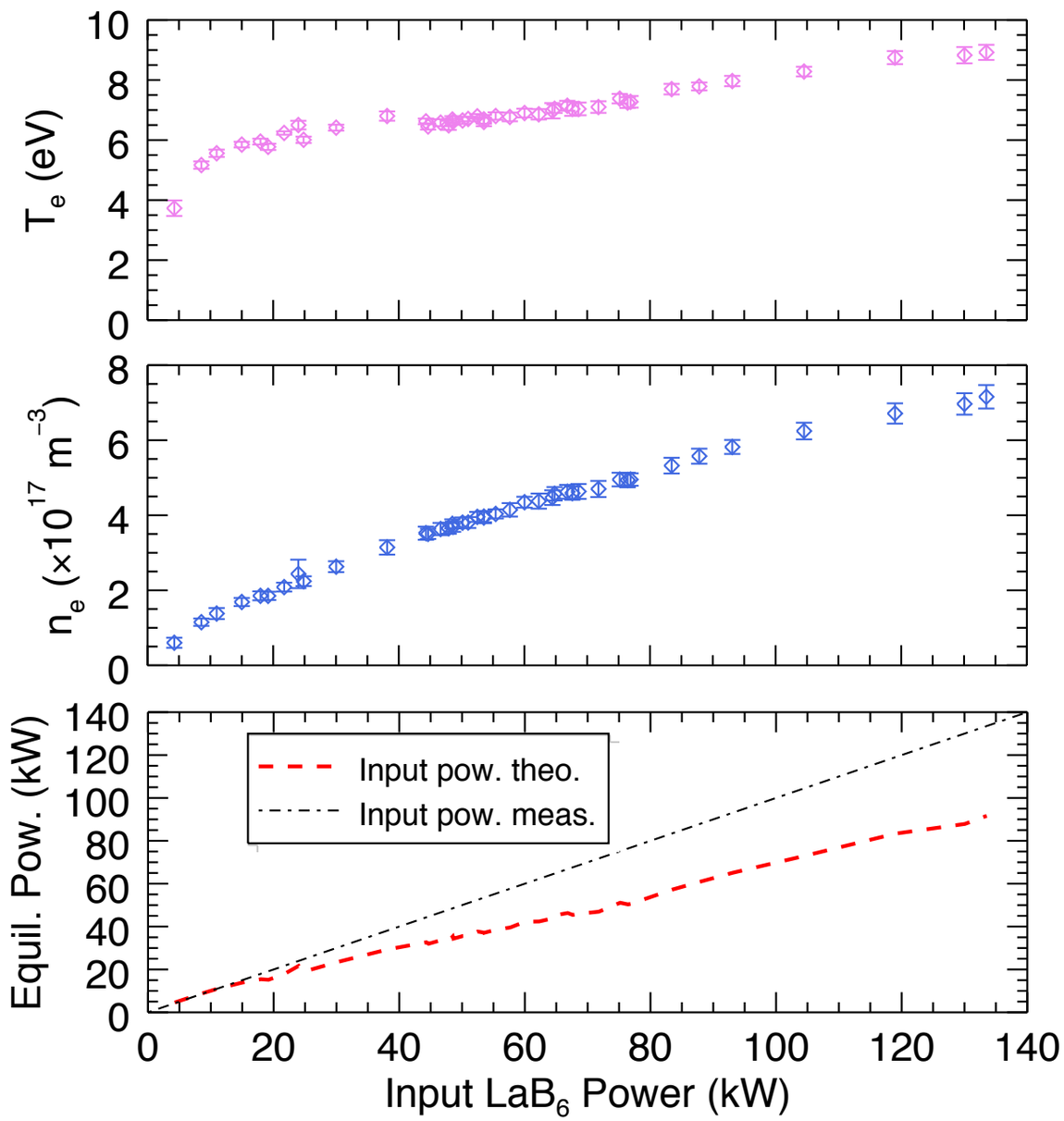

Scaling predicts plasma and dynamo parameter spaces

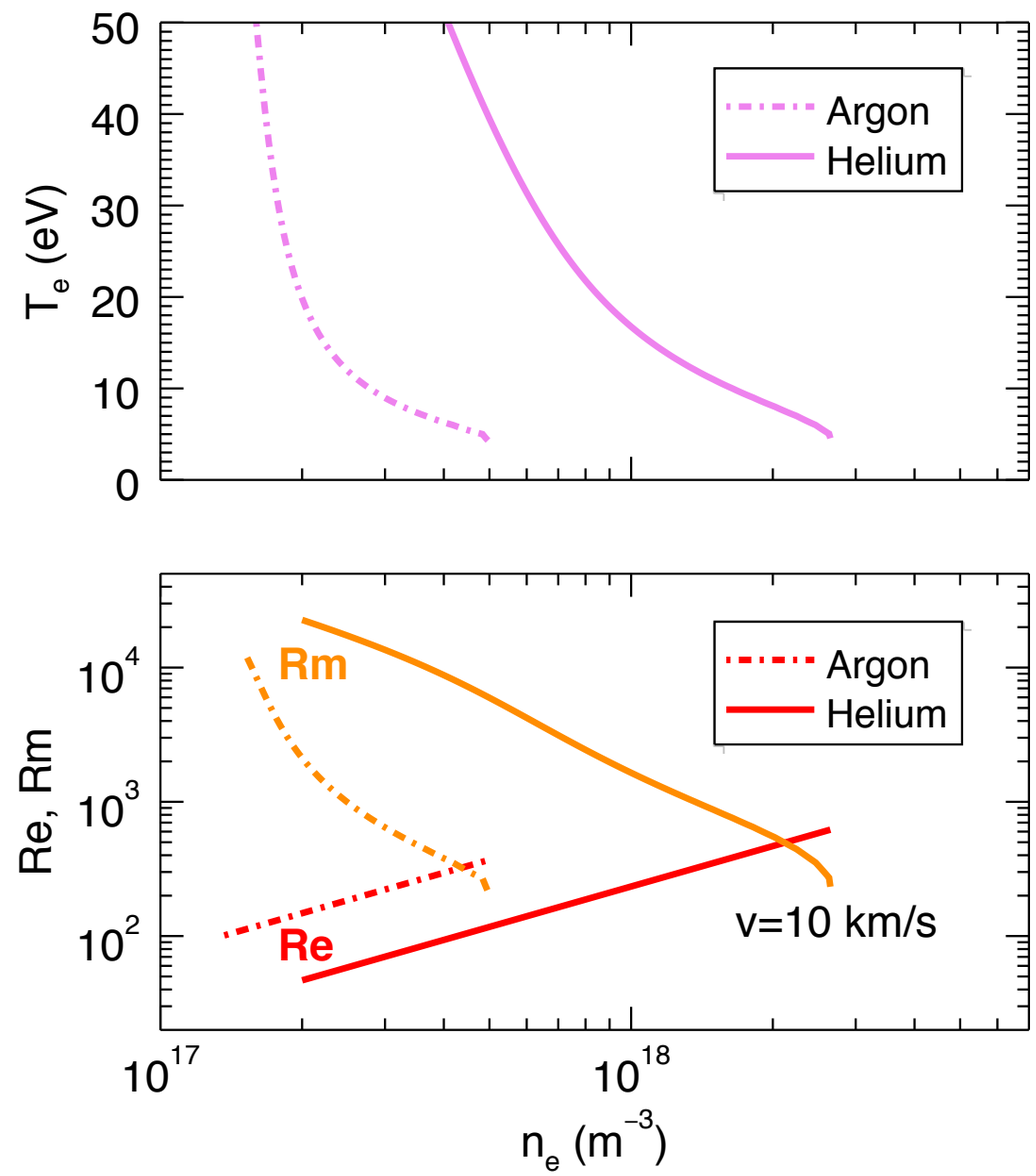

Time dependent flows are also feasible

- MPDX Galloway-Proctor Flow gives smooth but chaotic flow

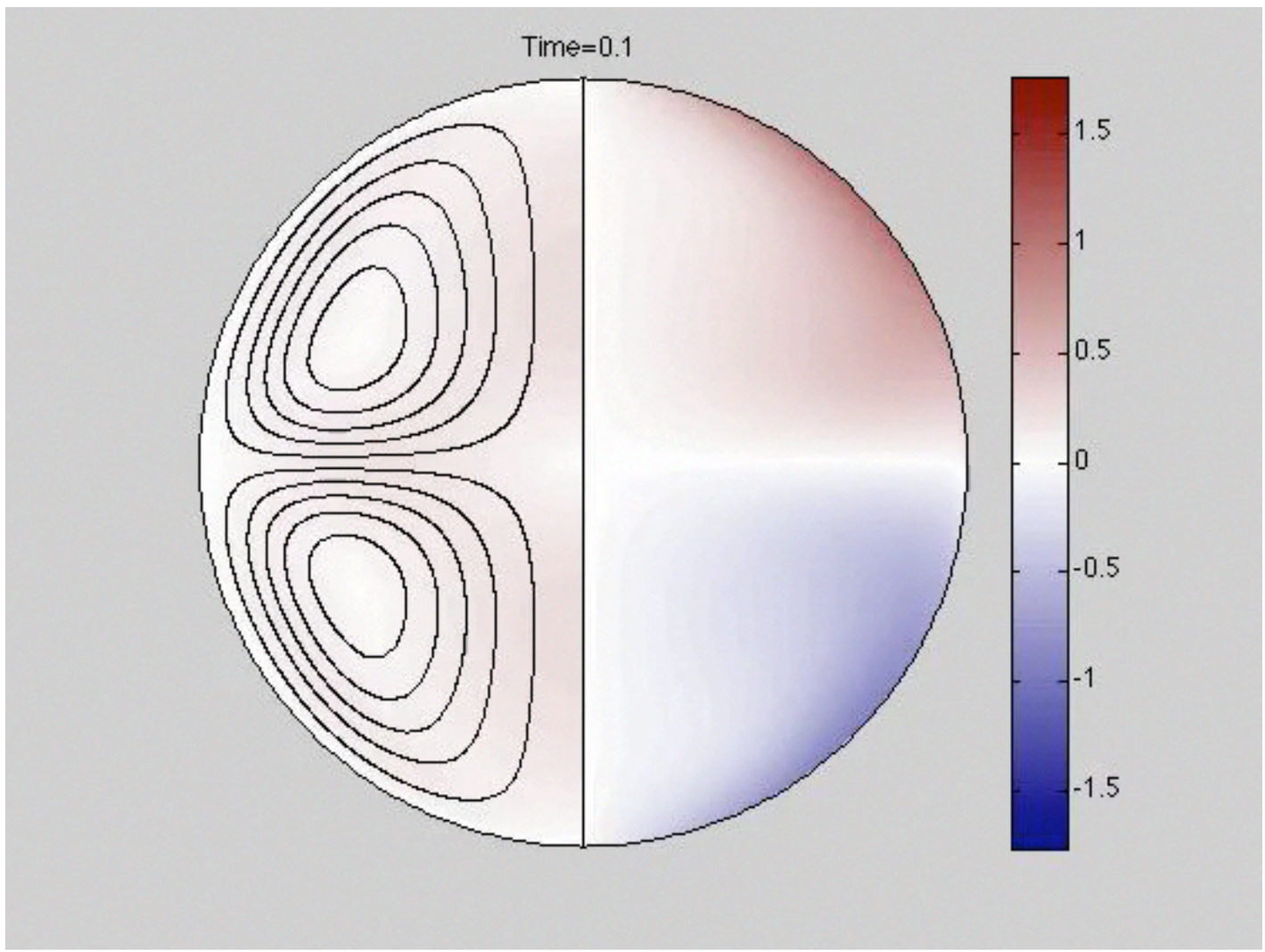

Chaos in time-periodic flow

- Boundary: Re=200, ω=0.6

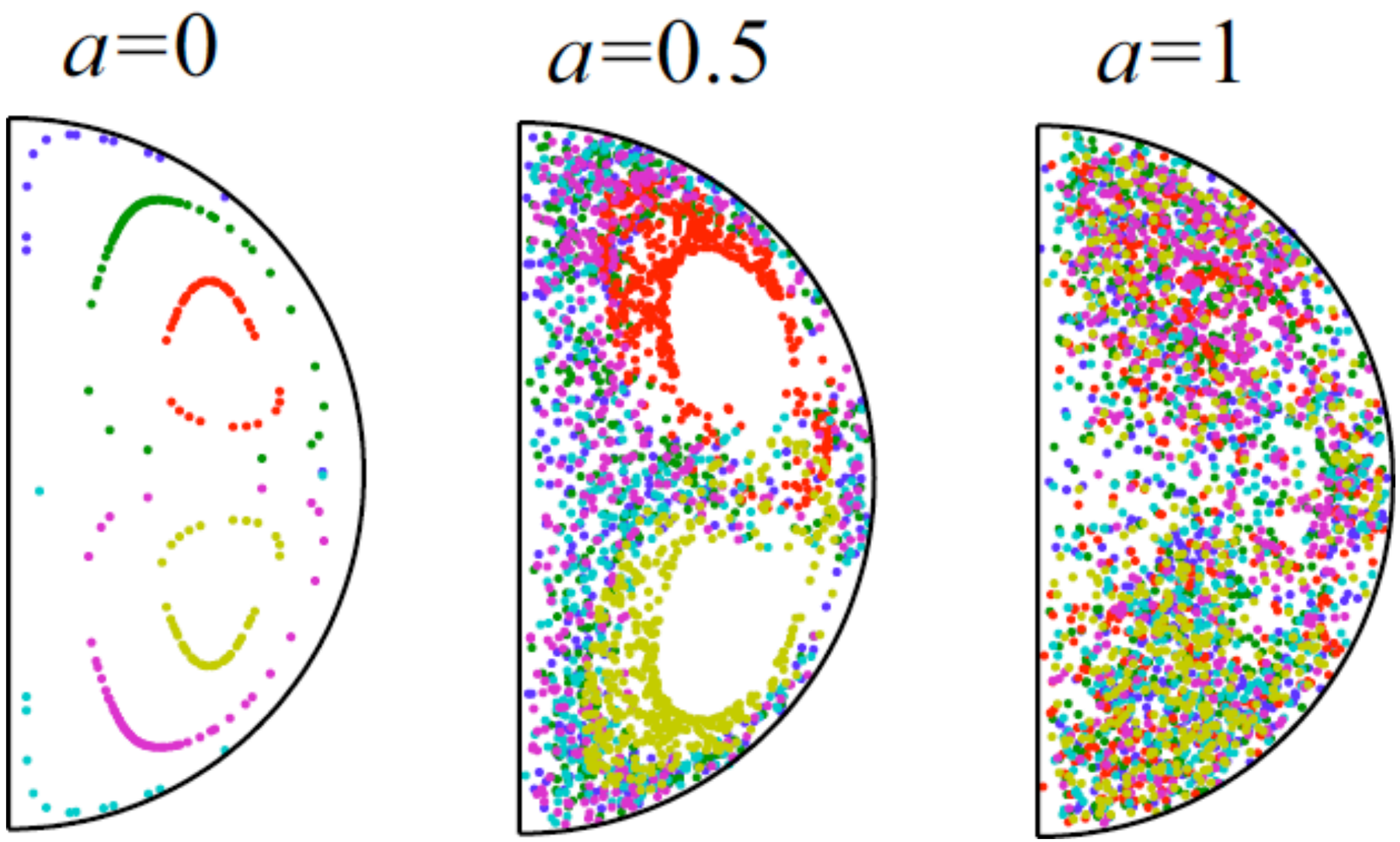

Fast Dynamos in spherical boundary-driven flows,
Phys. Rev. Lett. **111** 125001 (2013).

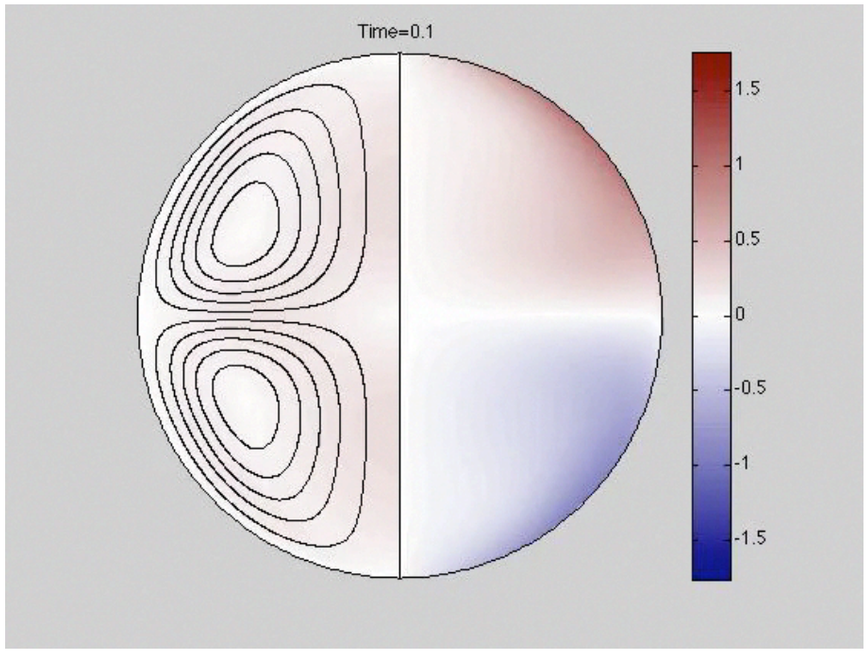

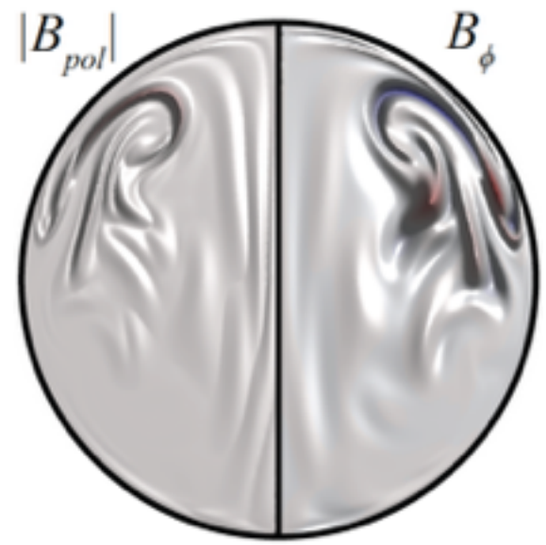

Dynamo growth rate

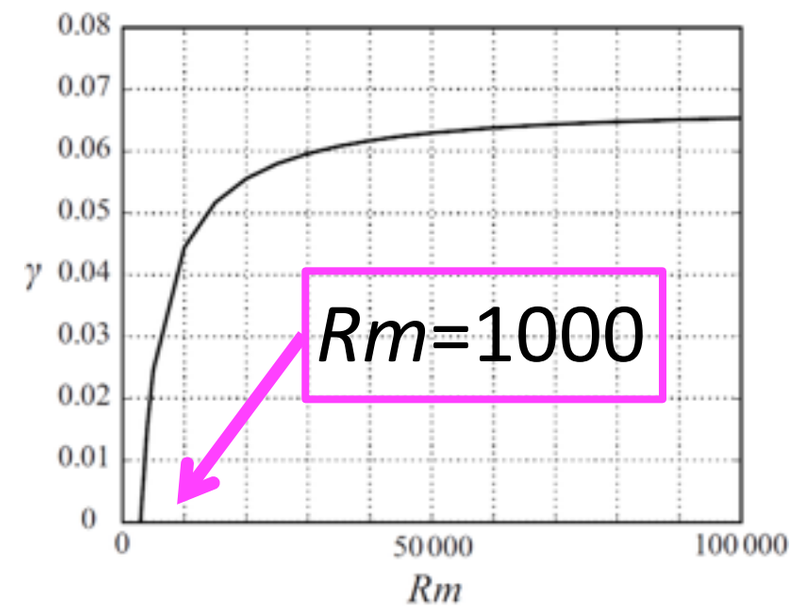

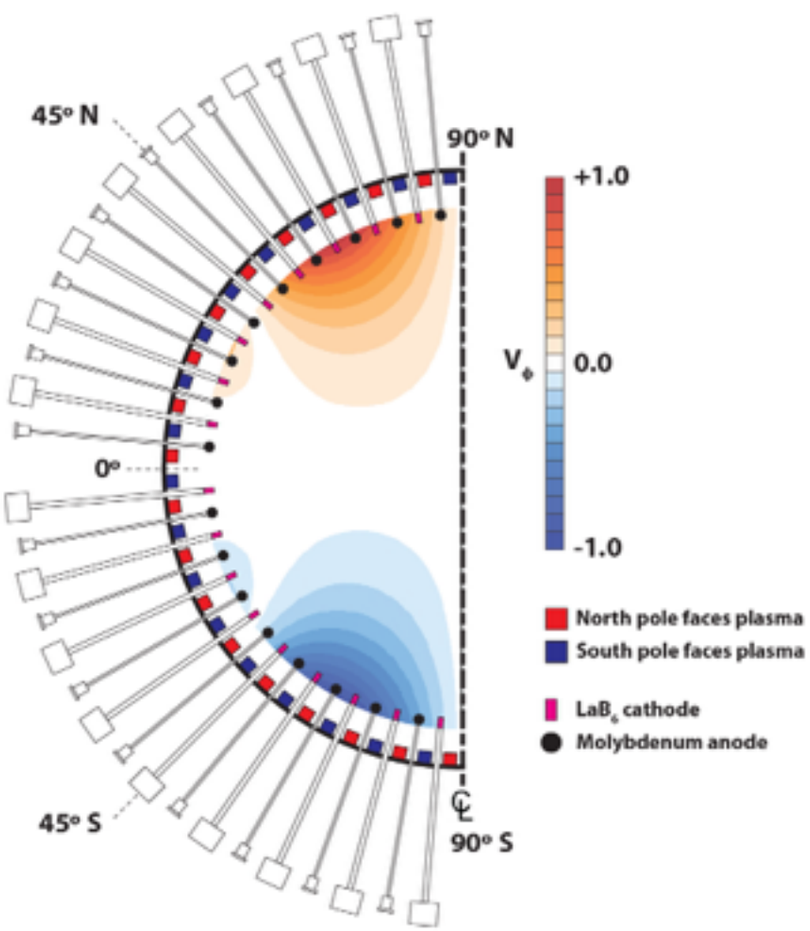

Galloway and Proctor type dynamo		
Re=100, Rm=1000		
Parameter	Argon	Helium
n	1X10	8X10
T	12	27
power (kW)	50	250
v	10	3
B	9	3
f_{drive}	637	191

Time dependent flows and LaB_6 bias set $v_\phi(\theta,t)$

Magnetized?

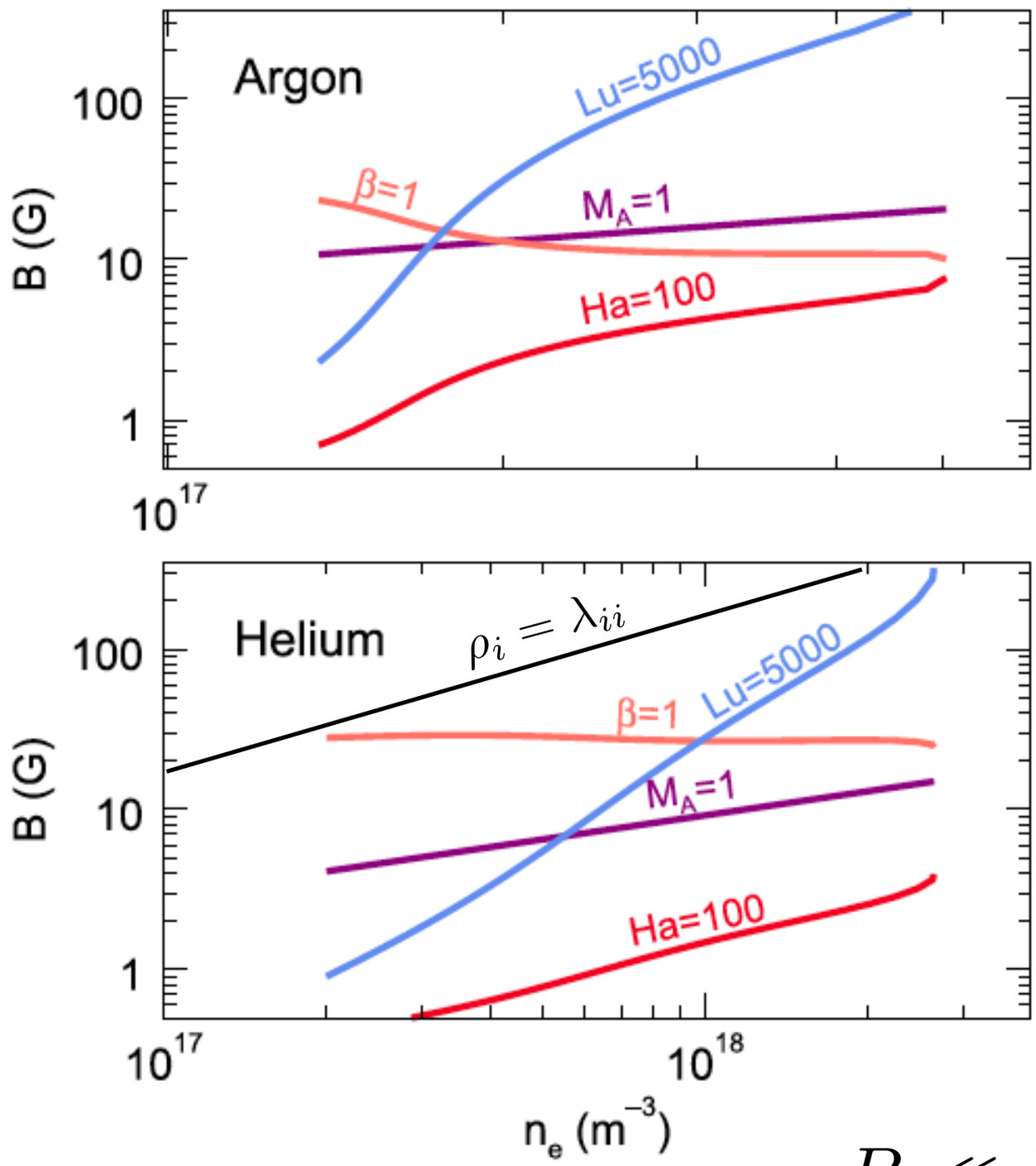

<u>isotropic vs anisotropic transport</u>

$$\rho_i \ll \lambda_{ii}$$

<u>viscous stronger than magnetic</u>
(Hartmann)

$$\sigma V B^2 \ll \nu \nabla^2 V$$

<u>large thermal energy</u>

$$\beta = \frac{2\mu_0 n(T_i + T_e)}{B^2} \gg 1$$

<u>kinetic energy dominated</u>

$$B \ll B_{equip} \text{ where } \frac{1}{2\mu_0} B_{equip}^2 = \frac{1}{2}\rho V^2$$

Helioseismology Experiment

Solar rotation profile

study angular momentum transport

use sound and MHD waves to measure flow

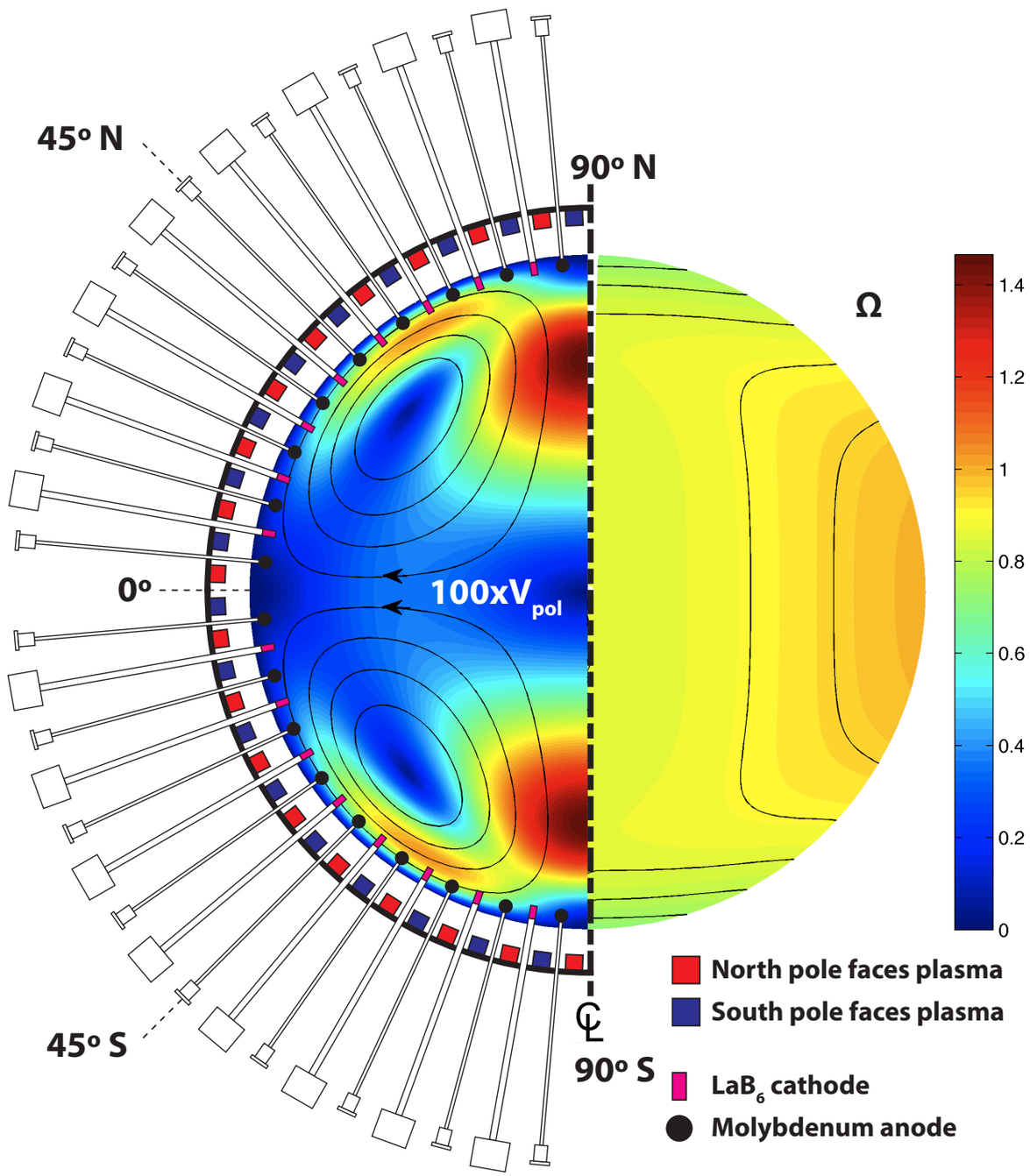

M=0 Toroidal Spectrum

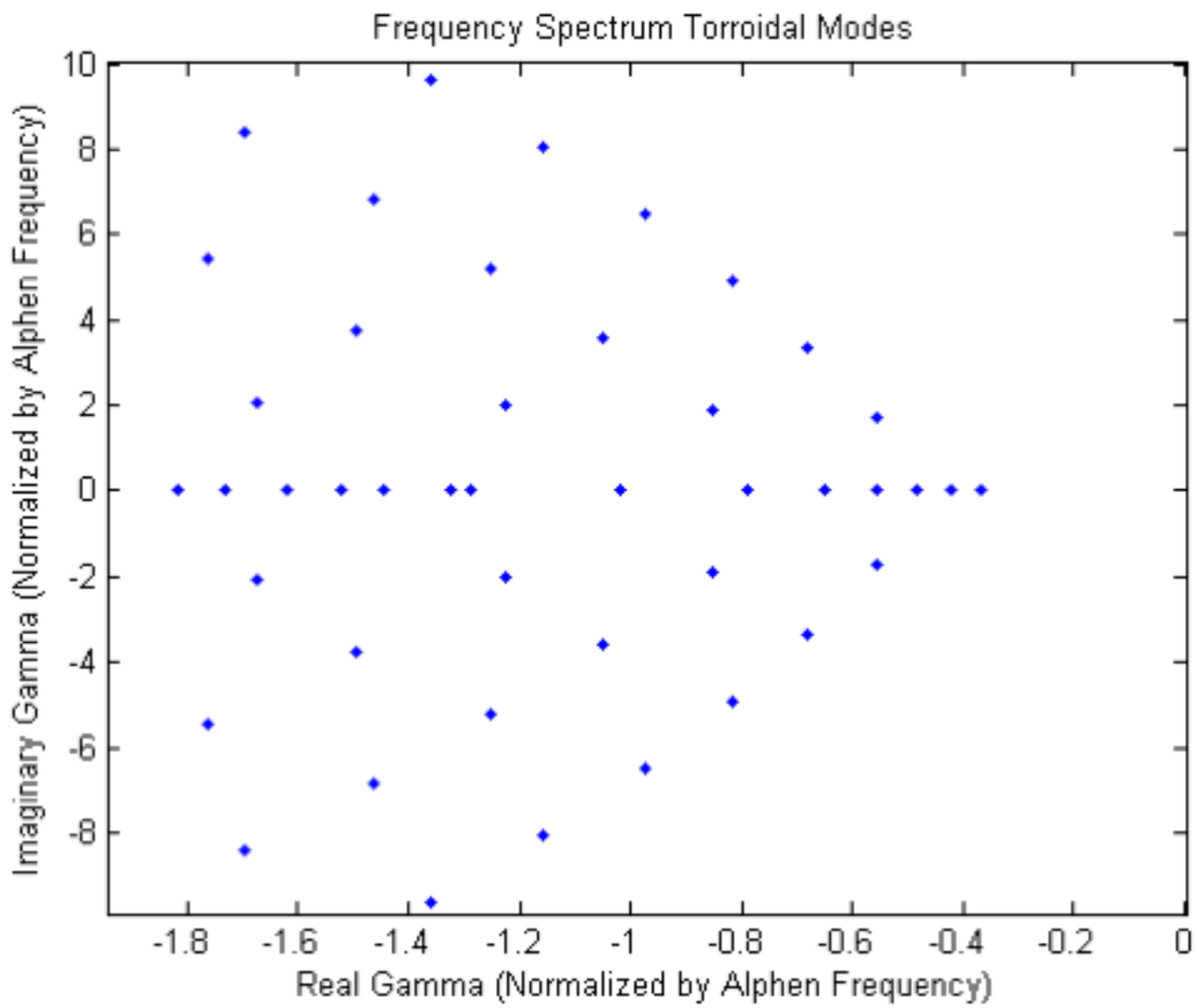

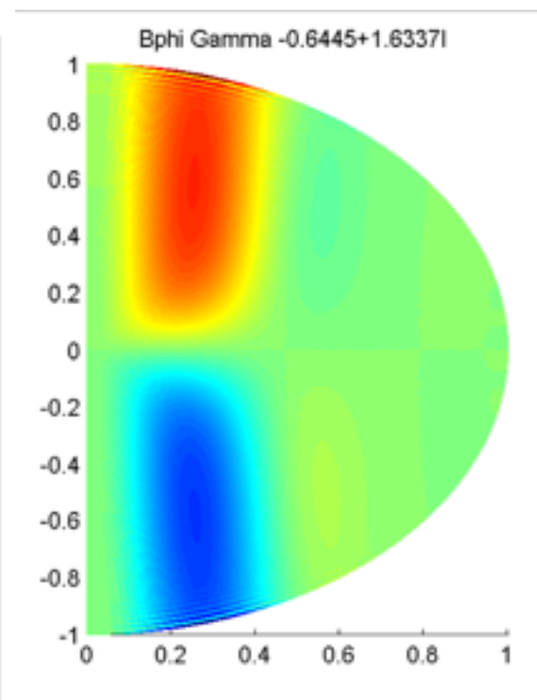

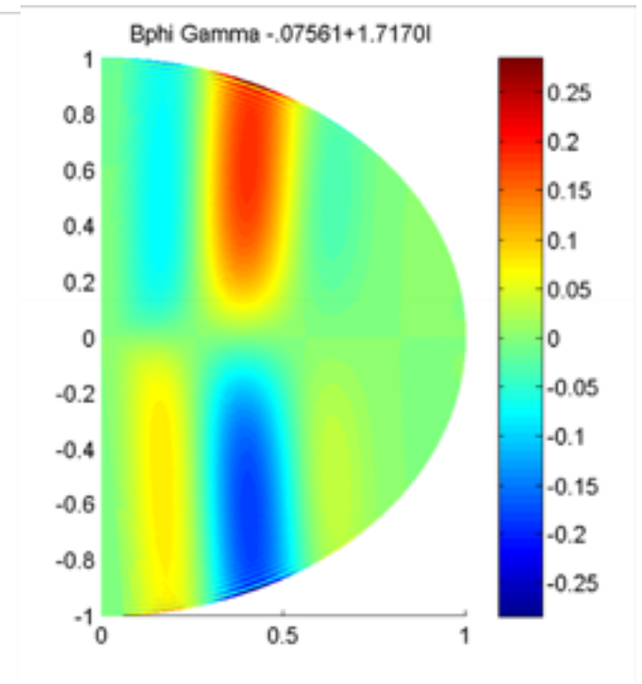

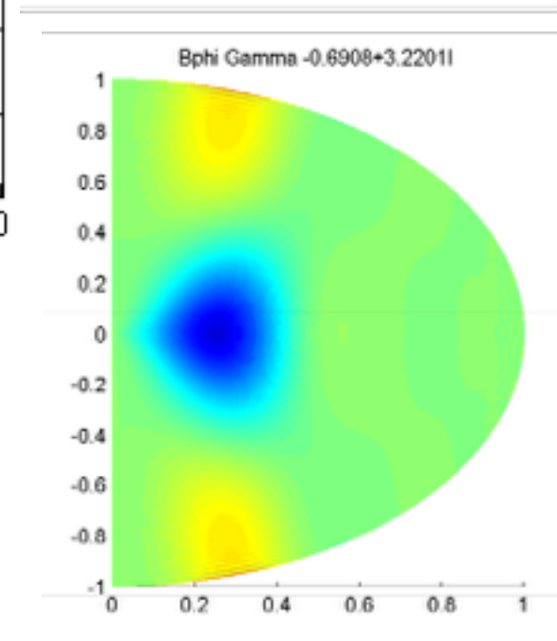

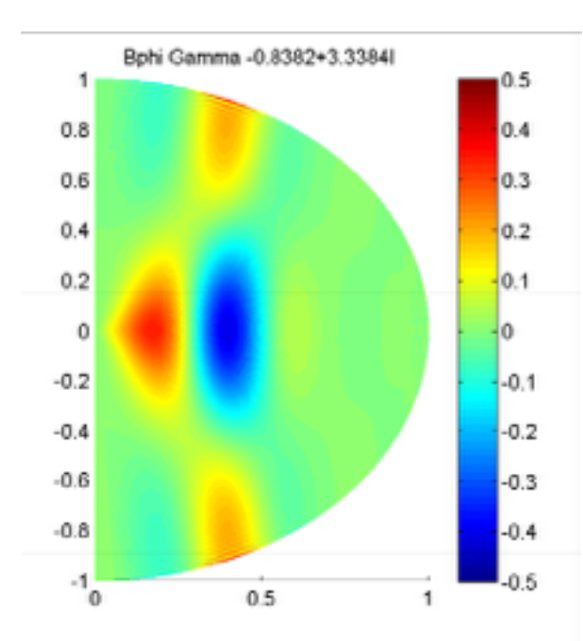

M=1 Modes

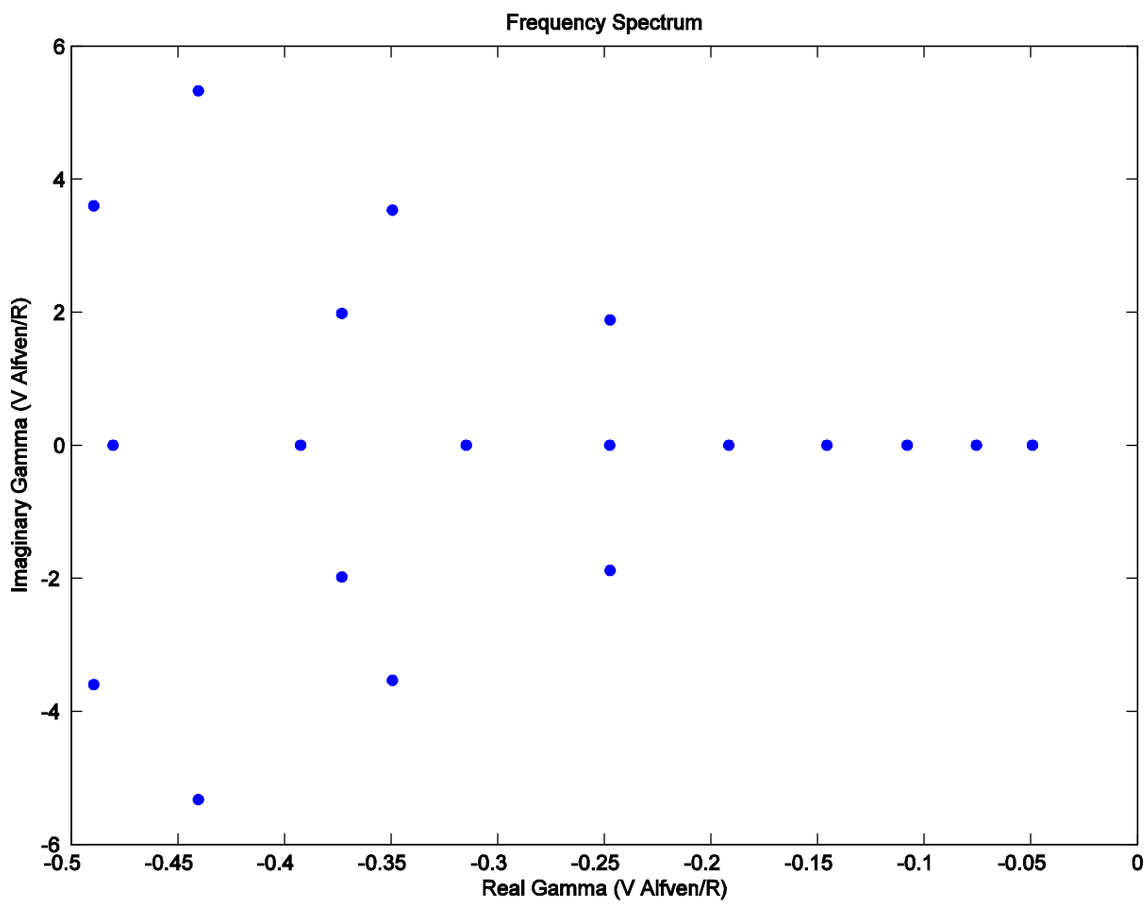
Frequency Spectrum
Imaginary Gamma (V Alfven/R)
Real Gamma (V Alfven/R)
6
4
2
0
-2
-4
-6
-0.5
-0.45
-0.4
-0.35
-0.3
-0.25
-0.2
-0.15
-0.1
-0.05
0

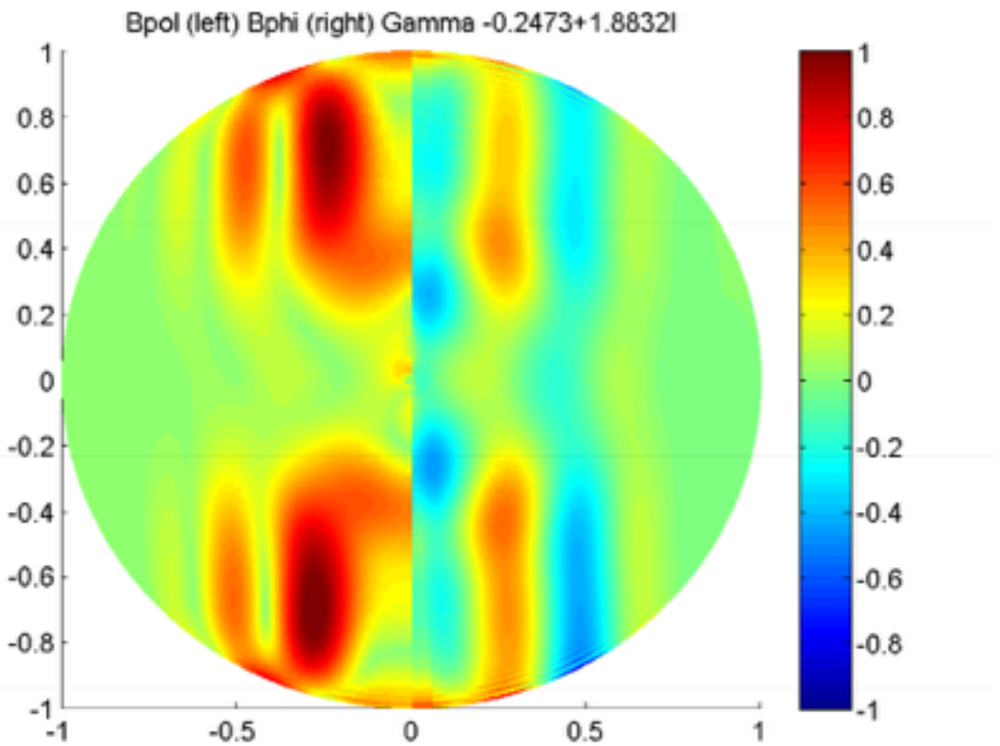
Bpol (left) Bphi (right) Gamma -0.2473+1.8832I
1
0.8
0.6
0.4
0.2
0
-0.2
-0.4
-0.6
-0.8
-1
-0.5
0
0.5
1

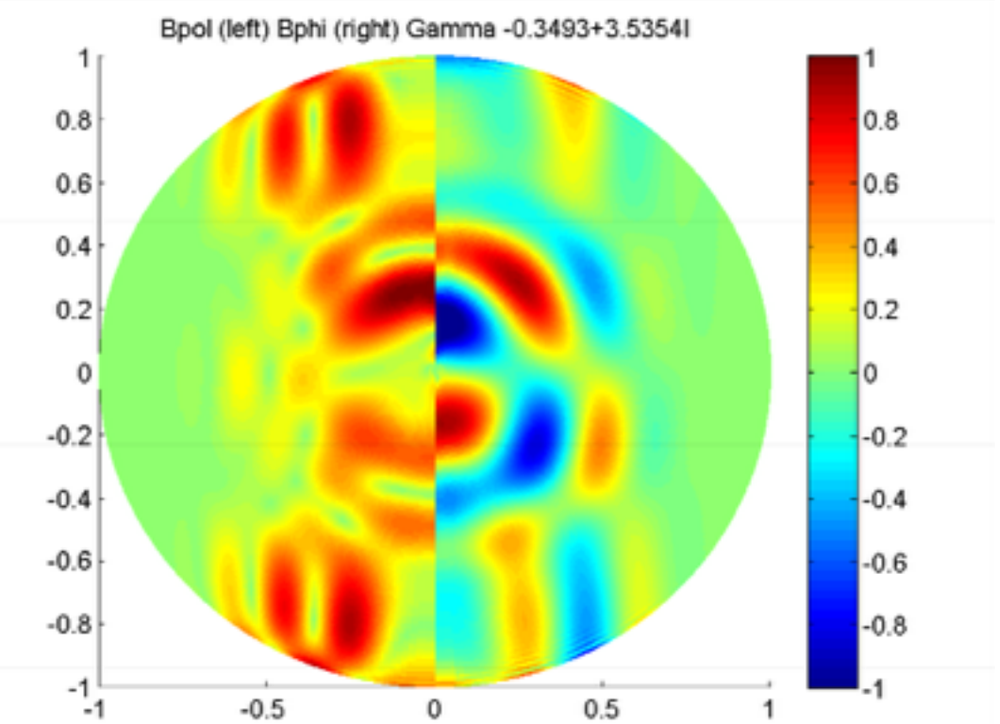
Bpol (left) Bphi (right) Gamma -0.3493+3.5354I
1
0.8
0.6
0.4
0.2
0
-0.2
-0.4
-0.6
-0.8
-1
-0.5
0
0.5
1

M=1 Modes with Velocity (0.5 Alfven Velocity)

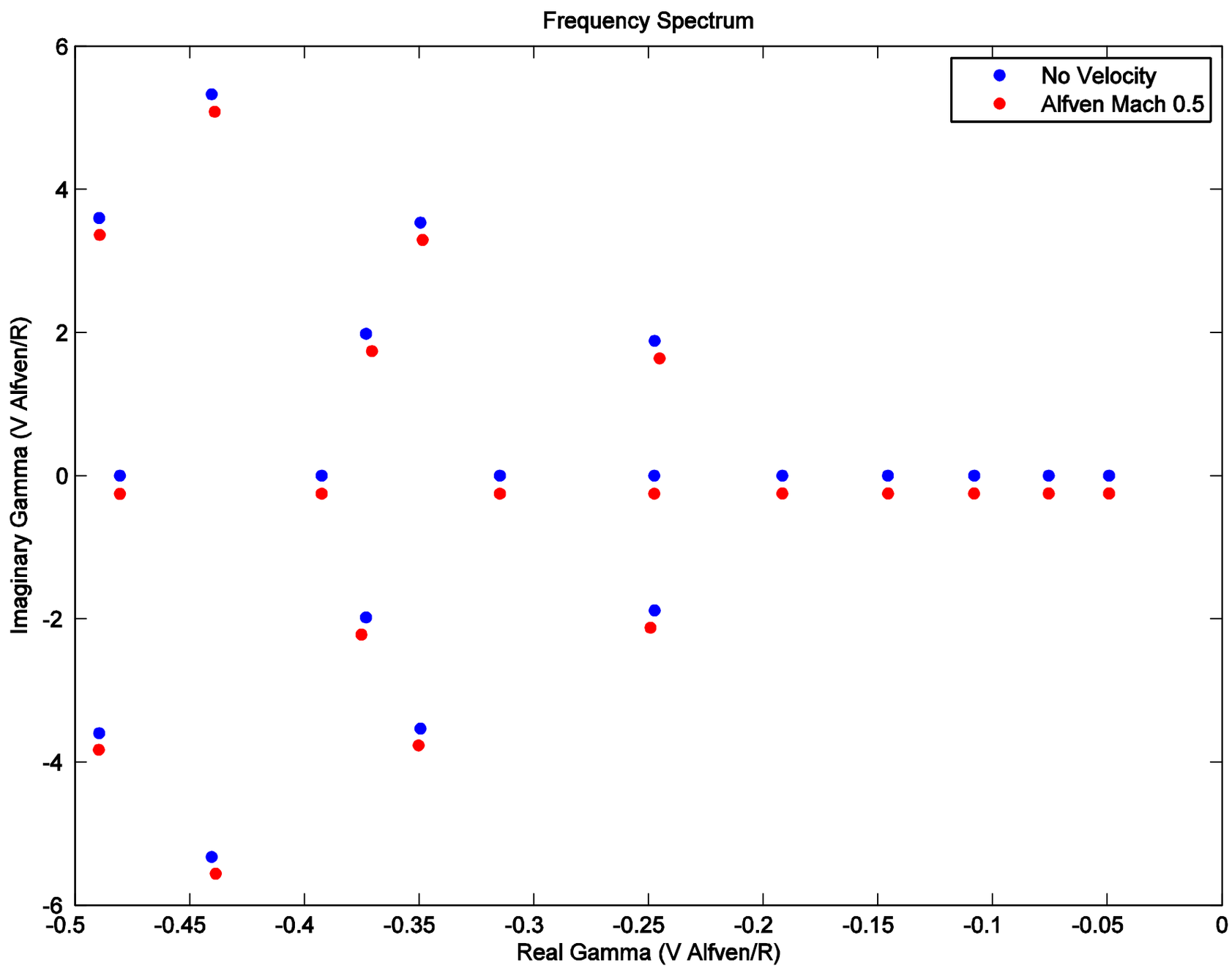

At low density, low collisionality plasma effects will play role

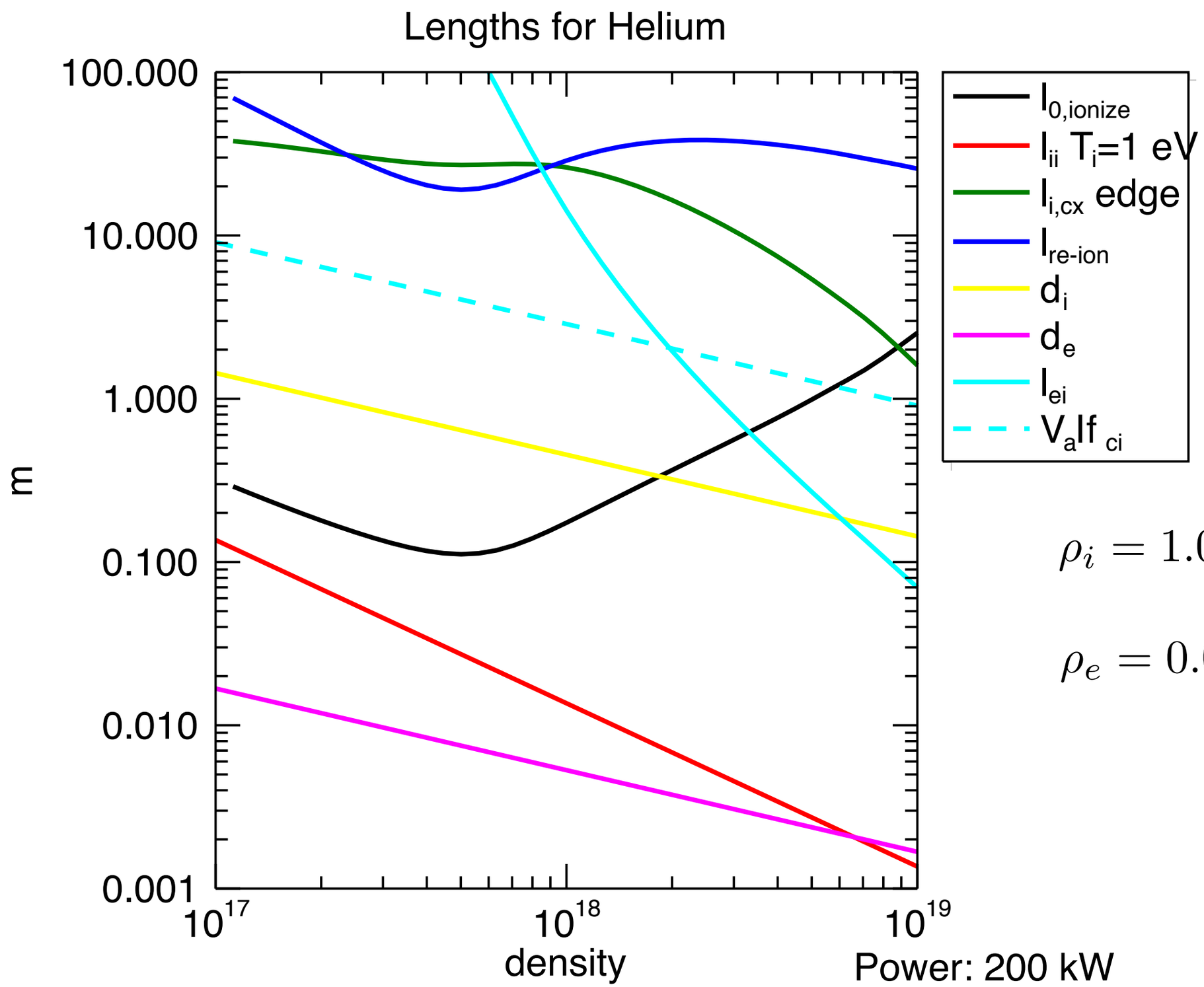

$$\rho_i = 1.02 \frac{\sqrt{\mu T_{\mathrm{i,eV}}}}{B_{\mathrm{g}}} \ \mathrm{m}$$

$$\rho_e = 0.023 \frac{\sqrt{T_{\mathrm{e,eV}}}}{B_{\mathrm{g}}} \ \mathrm{m}$$

Power: 200 kW

Speculative: *Laboratory Study of Magnetically Launched Stellar Winds*

Forest, Spitkovsky, Myers

CNC plasmas created with washer gun arrays

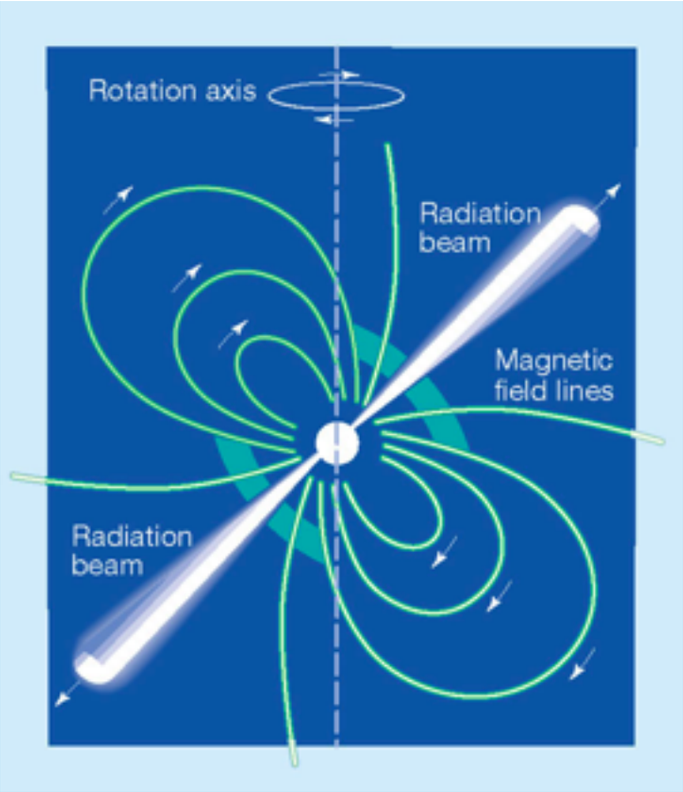

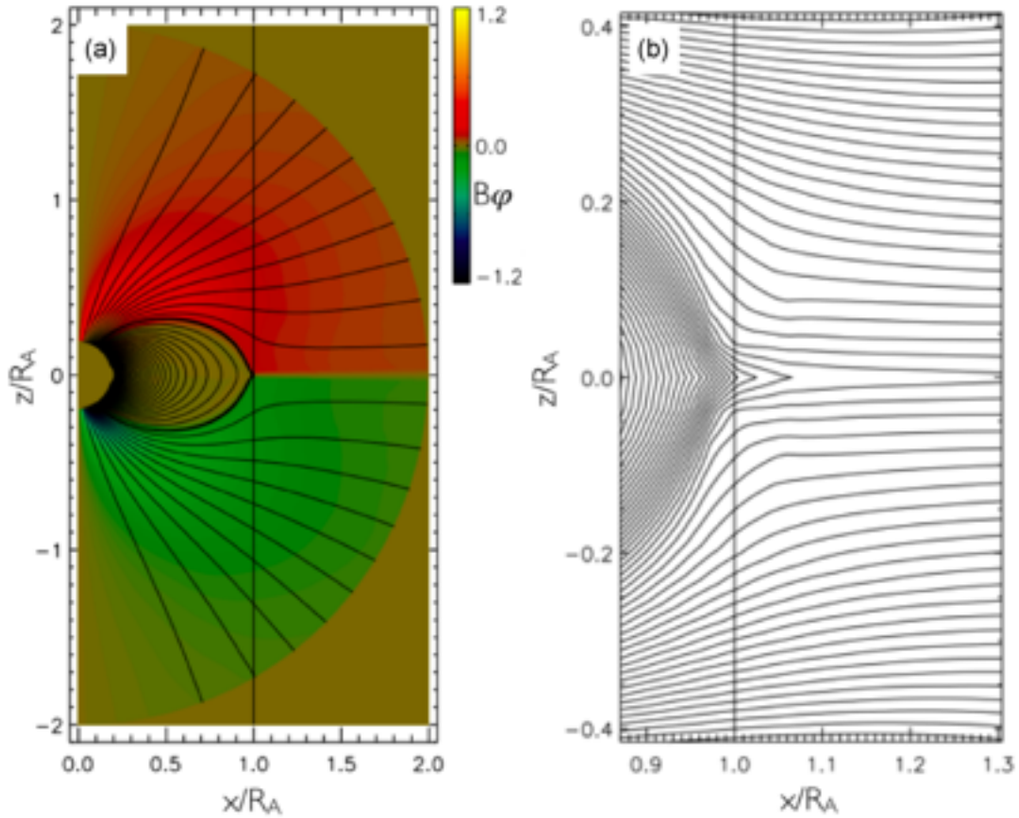

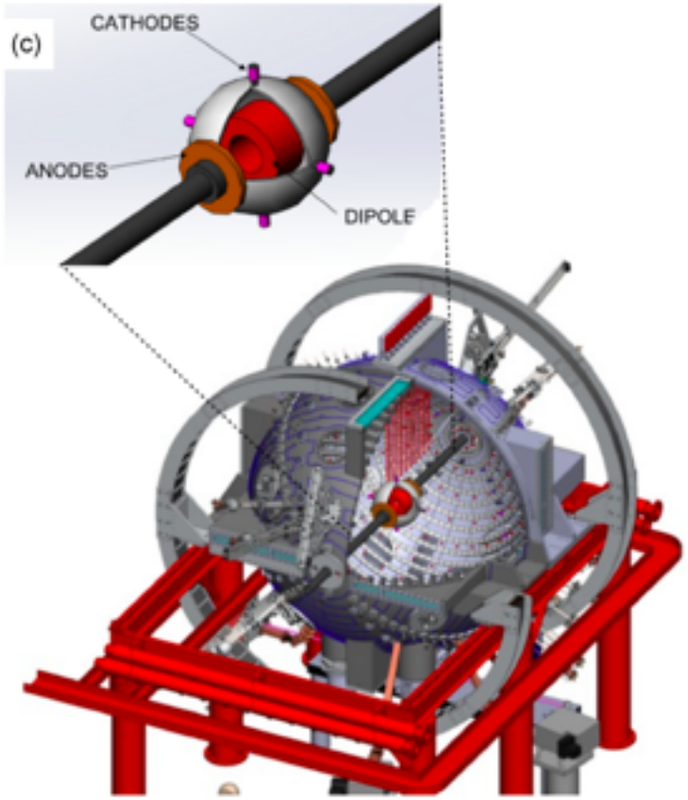

have the following key features:
1. The proxy star consists of an insulating sphere that houses either permanent magnets or phased magnetic
coils that produce an astrophysically relevant potential (vacuum) magnetic field configuration.
2. Emissive cathodes mounted on the equator of the proxy star serve as the primary plasma source.
3. Anodes mounted on the poles of the proxy star are biased with respect to the equatorial cathodes in
order to generate EB rotation in the source plasma and launch the stellar wind.
4. The centrifugally driven wind will be magnetically dominated until the so-called Alfv´en point (radius)
where the kinetic energy of the plasma exceeds the energy in the magnetic field.
5. Flexibility in the design of the proxy star will permit the creation of winds emanating from both
aligned and oblique rotators, thereby broadening the range of physical processes that can be studied.

Scientific Objectives:
1. Analysis of the global magnetic topology: Closed field lines are expected inside of the Alfv´en point, while the outer, flow-dominated regions of the plasma are expected to have an open field configuration. Measurements of these closed and open field regions as well as of the flow-driven conversion of poloidal to toroidal magnetic field in the open field regions are of great astrophysical interest.
2. Steady-state driven reconnection: At the equatorial transition between the closed and open field regions, a Y-point is formed where the outflowing magnetized plasma continuously undergoes magnetic reconnection. We will probe both the magnetic and kinetic aspects of this steady-state driven reconnection process, including possible plasmoid generation and particle acceleration and heating.
3. Undulating current sheets: The oblique rotator configuration will produce an undulating current sheet that is similar to the heliospheric current sheet generated by the solar wind. The resulting alternating field sectors rotating in the equatorial plane are of keen interest given that they can trigger transient events such as day-side reconnection in the Earth's magnetosphere.
4. Quantified energy and momentum fluxes: By measuring the magnetic and kinetic properties of the laboratory wind at different radii, we can quantify the flow of energy and momentum away from the proxy star. This will contribute to the understanding of how stellar winds extract energy and angular momentum from their source stars (i.e., the "spin down" problem).
5. Comparison to numerical simulations: The proposed experiments will be numerically simulated using the TRISTAN-MP particle-in-cell (PIC) code, which is typically used to simulate the dynamics of pulsar winds. Comparing the laboratory and simulation results will help to interpret the observed

Reconnection setup in TREX

Insert holding field coils

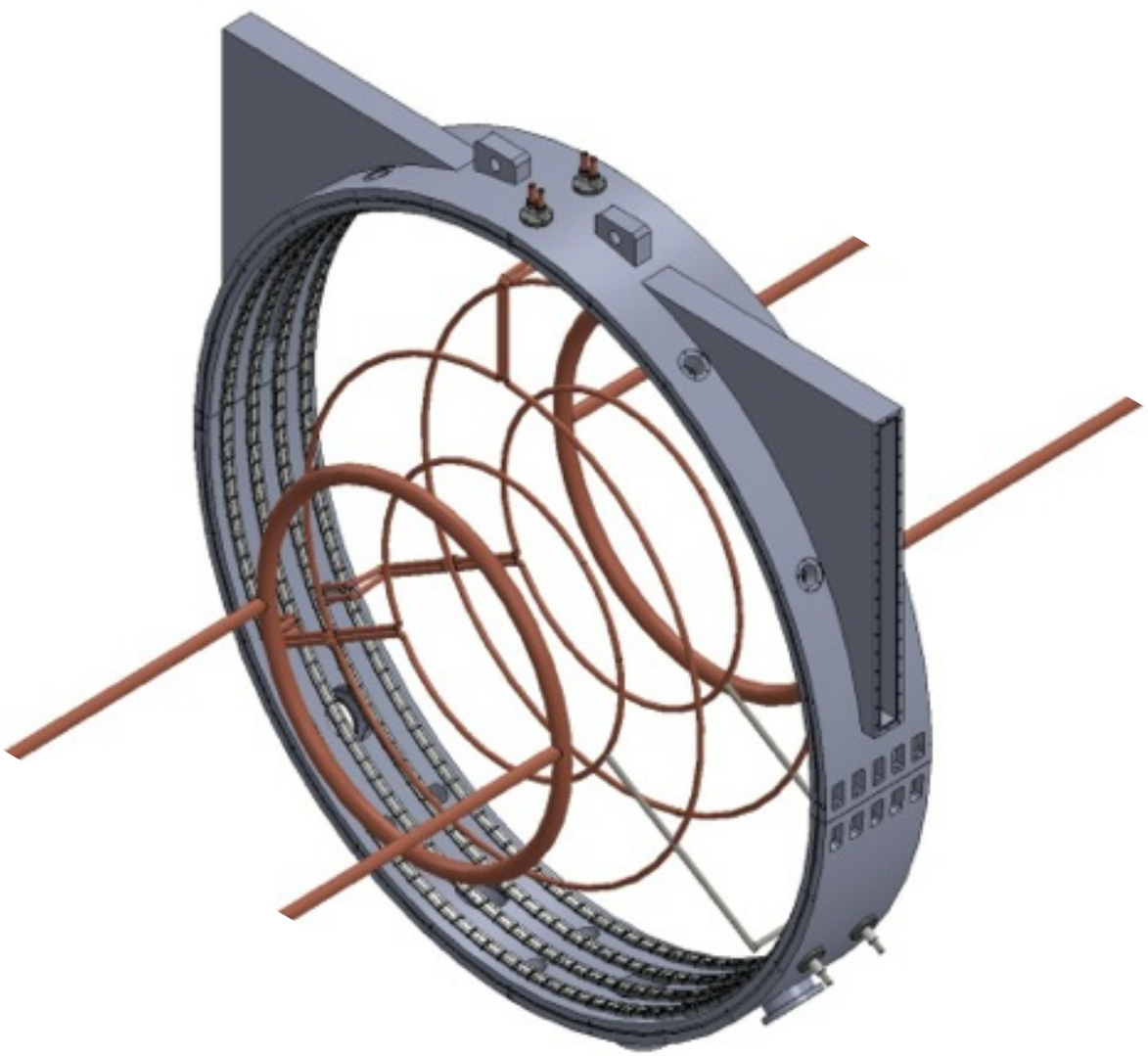

MPDX (just delivered)

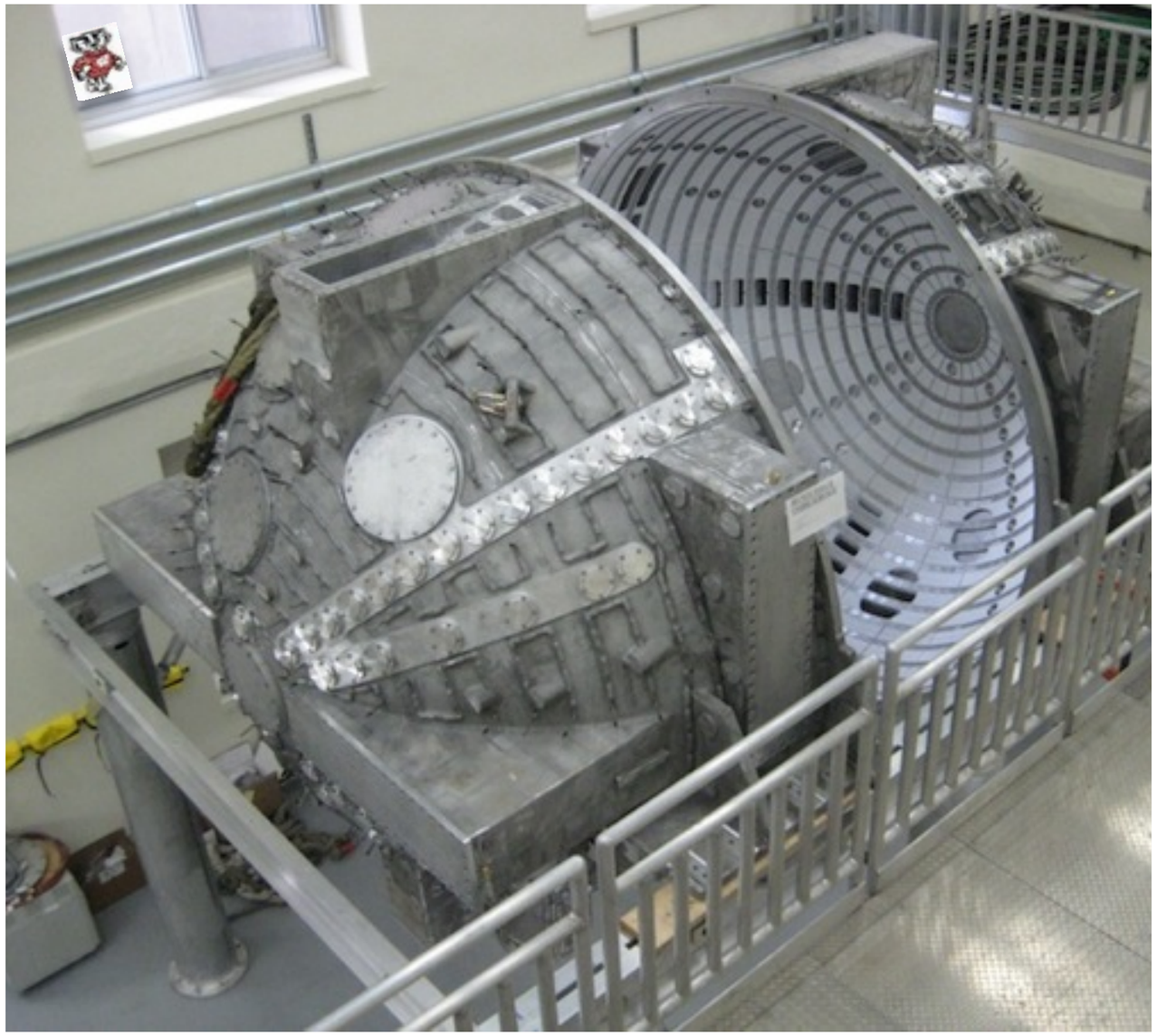

Reconnection setup in TREX

TF coils & TREX-insert for reconnection

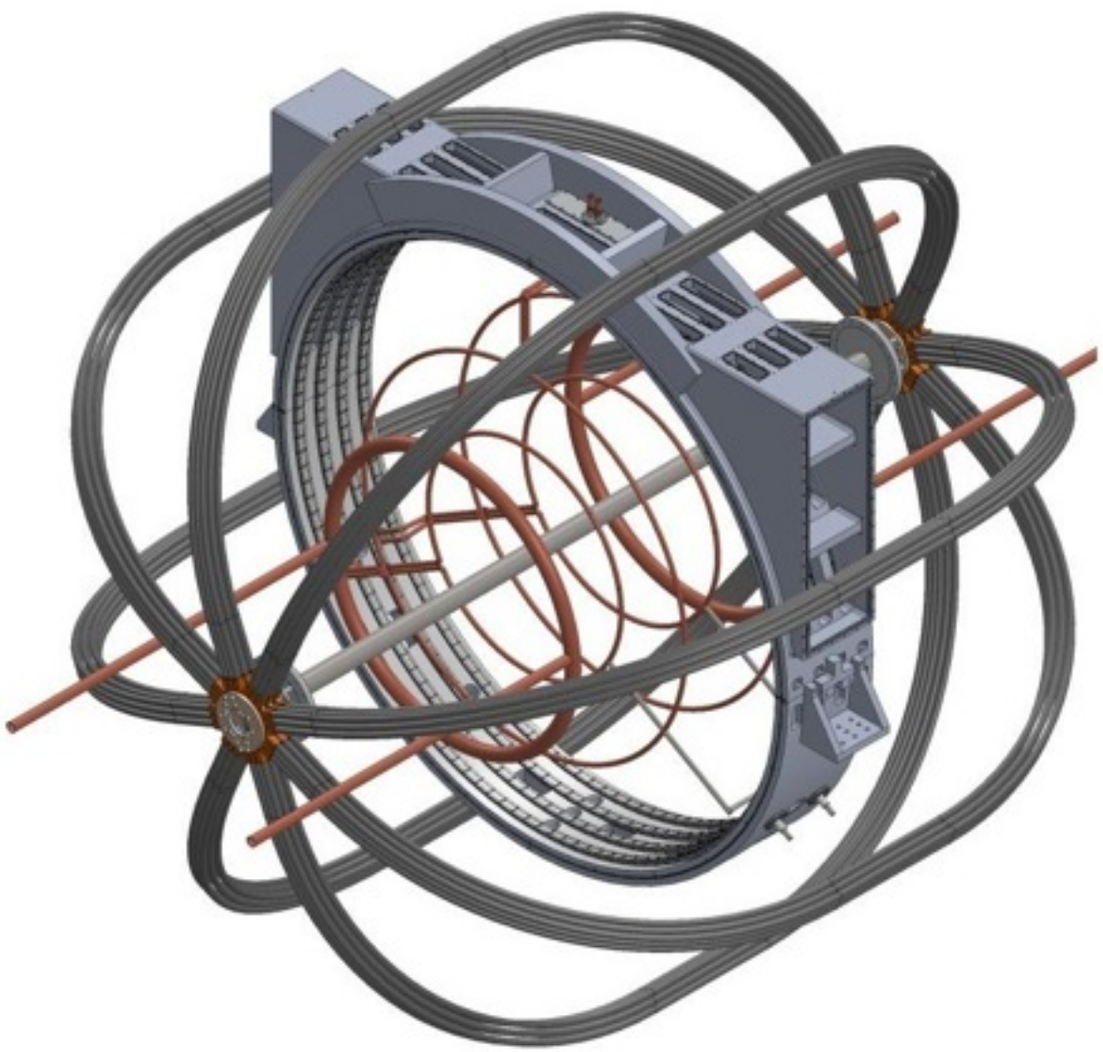

MPDX with TREX hardware

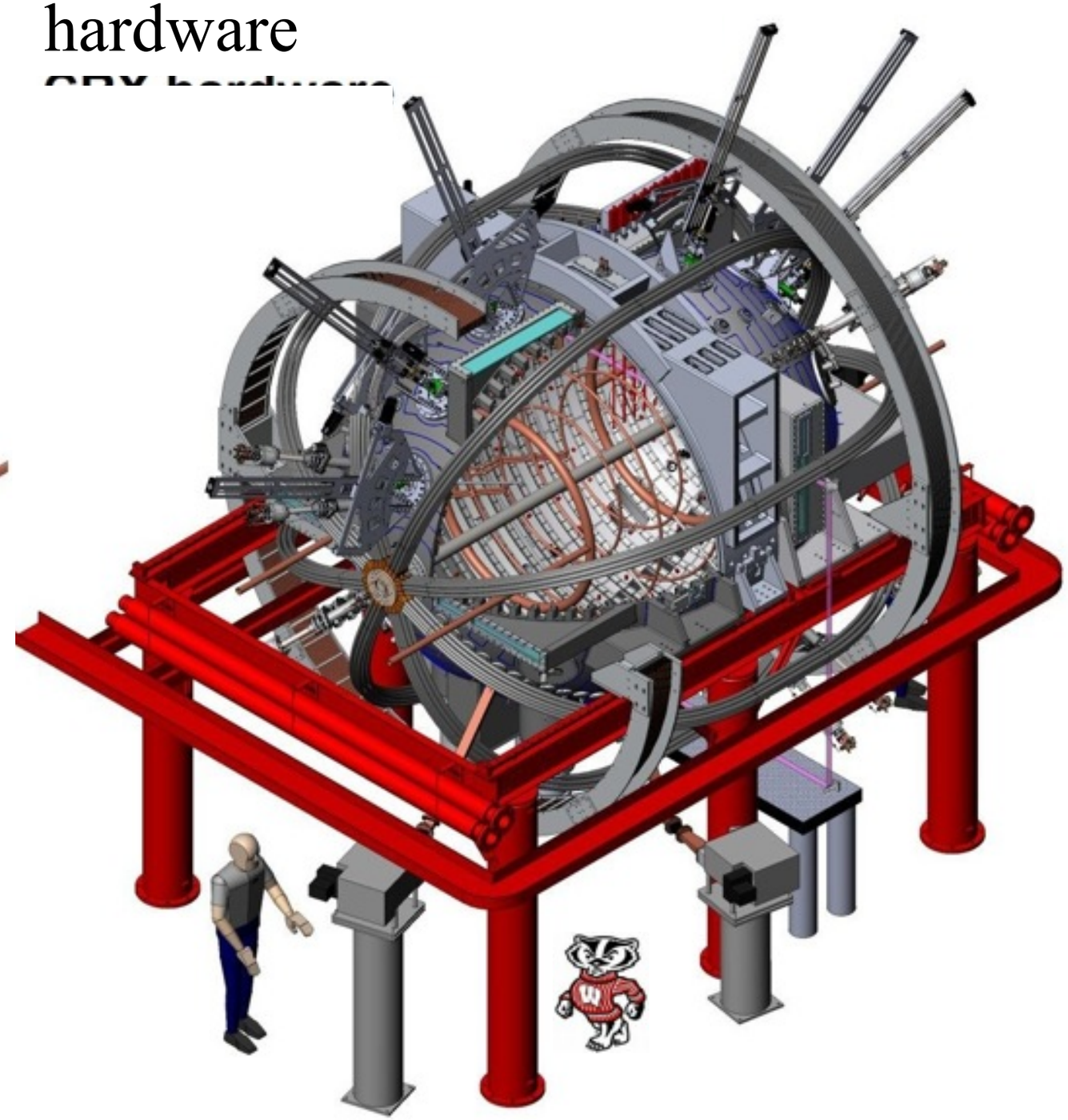

Key new hardware

- Helmholtz Coils
  - 2 × 80 turns, CW, 800A
    ➔ B ~ 0.025T
- TF coil
  - 96 turns,
  - CW, 800A, ➔ B= 0.015 T @ R=1m
  - Pulsed, 13kA ➔ B = 0.25 T @ R=1m
- Poloidal field coils
  - 2 × 20 turns, pulsed, 5kA
    ➔ B ~ 0.04T
- Reconnection drive coils
  - 2 × 1 turns, 5kV, 10kA

MPDX with TREX hardware

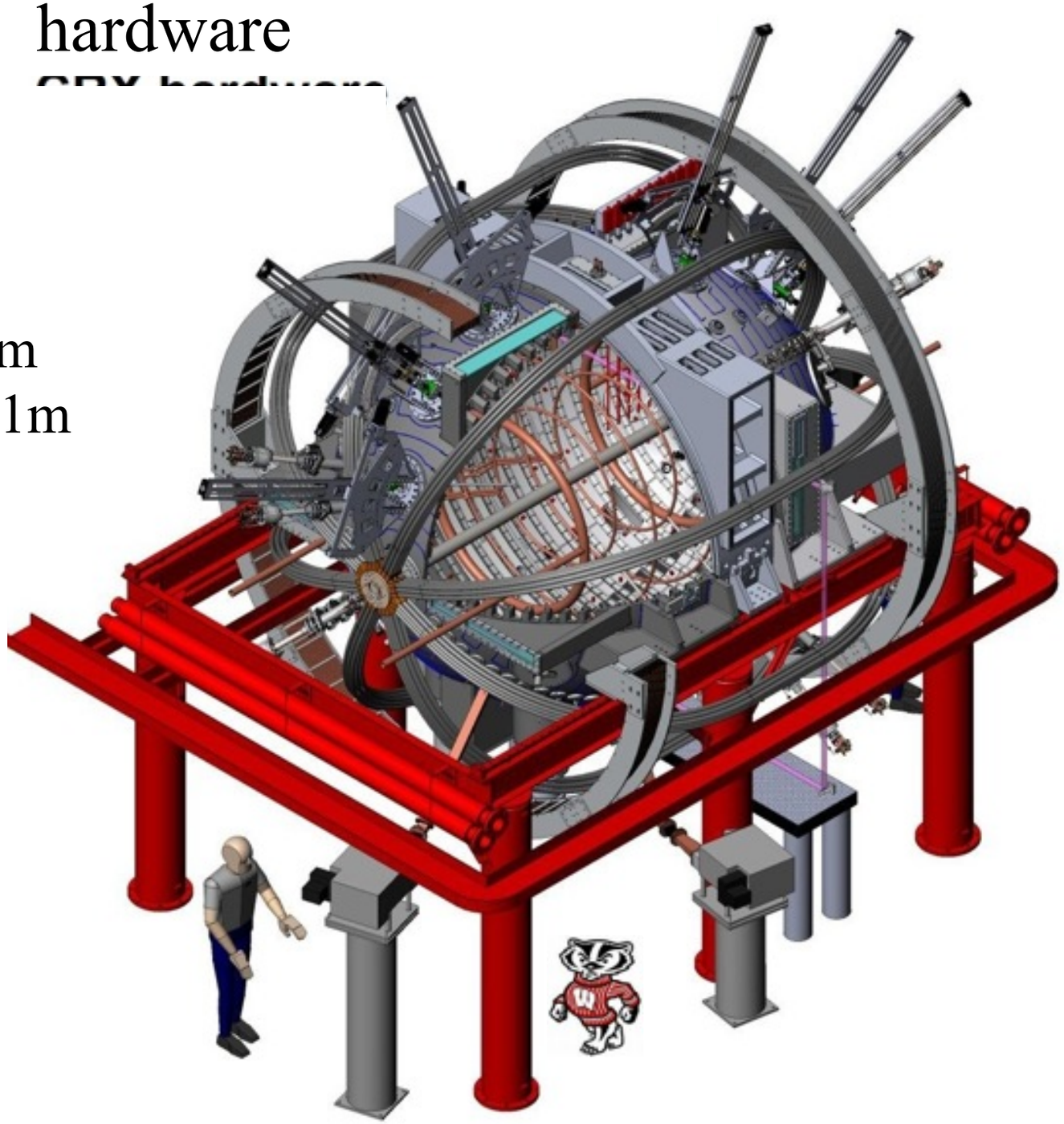

Role of Collisions, Moderate Guide-field Reconnection

- Continuous operation of magnetic coils
- Plasma pulsed at 1Hz
- $B_g = 20$ mT at 1m

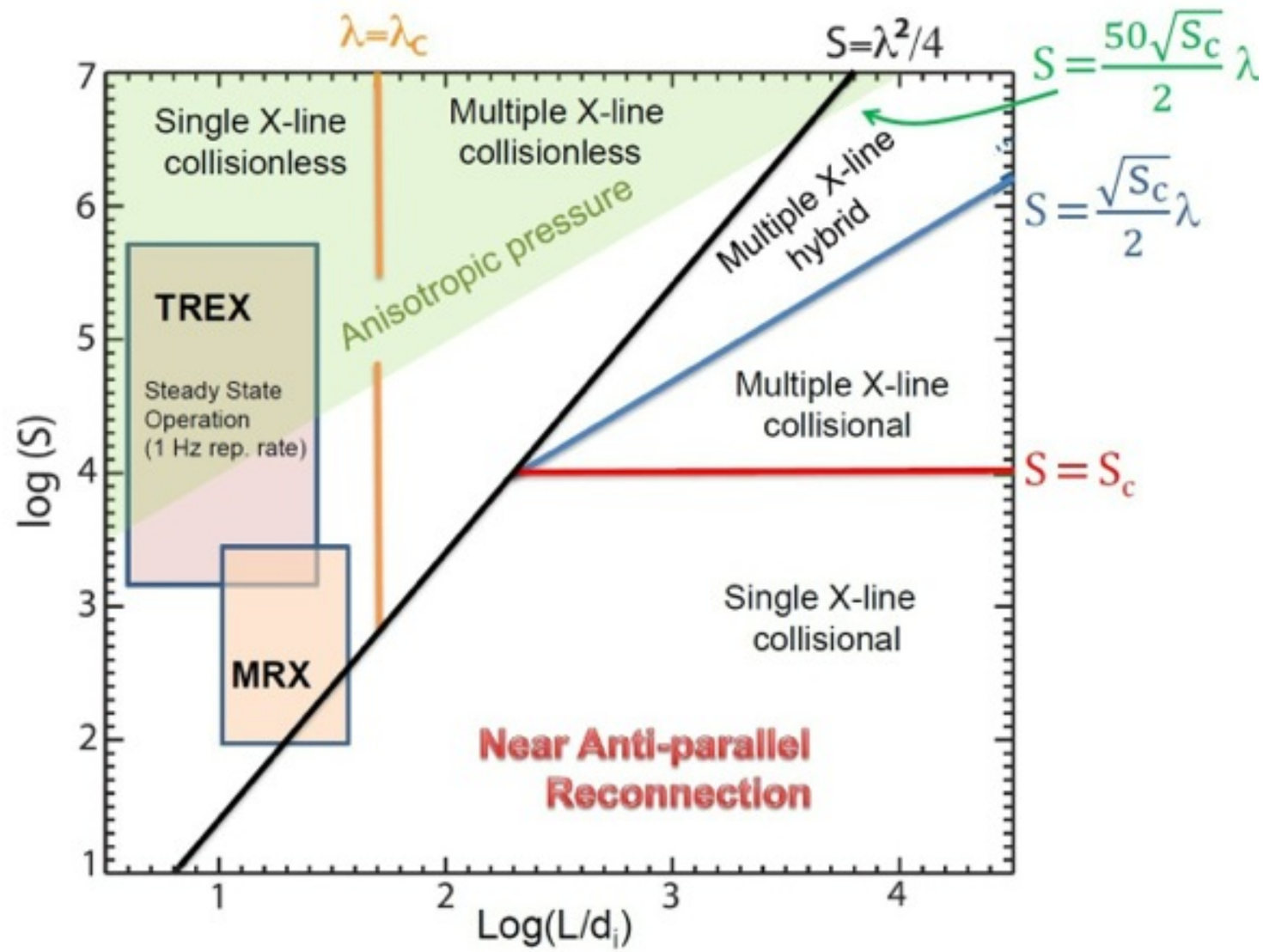

	$n_e/[10^{18}\ m^{-3}]$	$T_e/[eV]$	$B_r/[T]$	$B_g/[T]$	L/[m]
CRX	0.1-10	8 – 40	0.04	0 – 0.3	0.8 – 1.8
MRX	10 – 100	5 – 10	0.03	0 – 0.1	0.7
VTF	0.1-1	8 – 30	0.01	0.1	0.3

Symmetric Inflow Configuration

TREX, poloidal magnetic fields

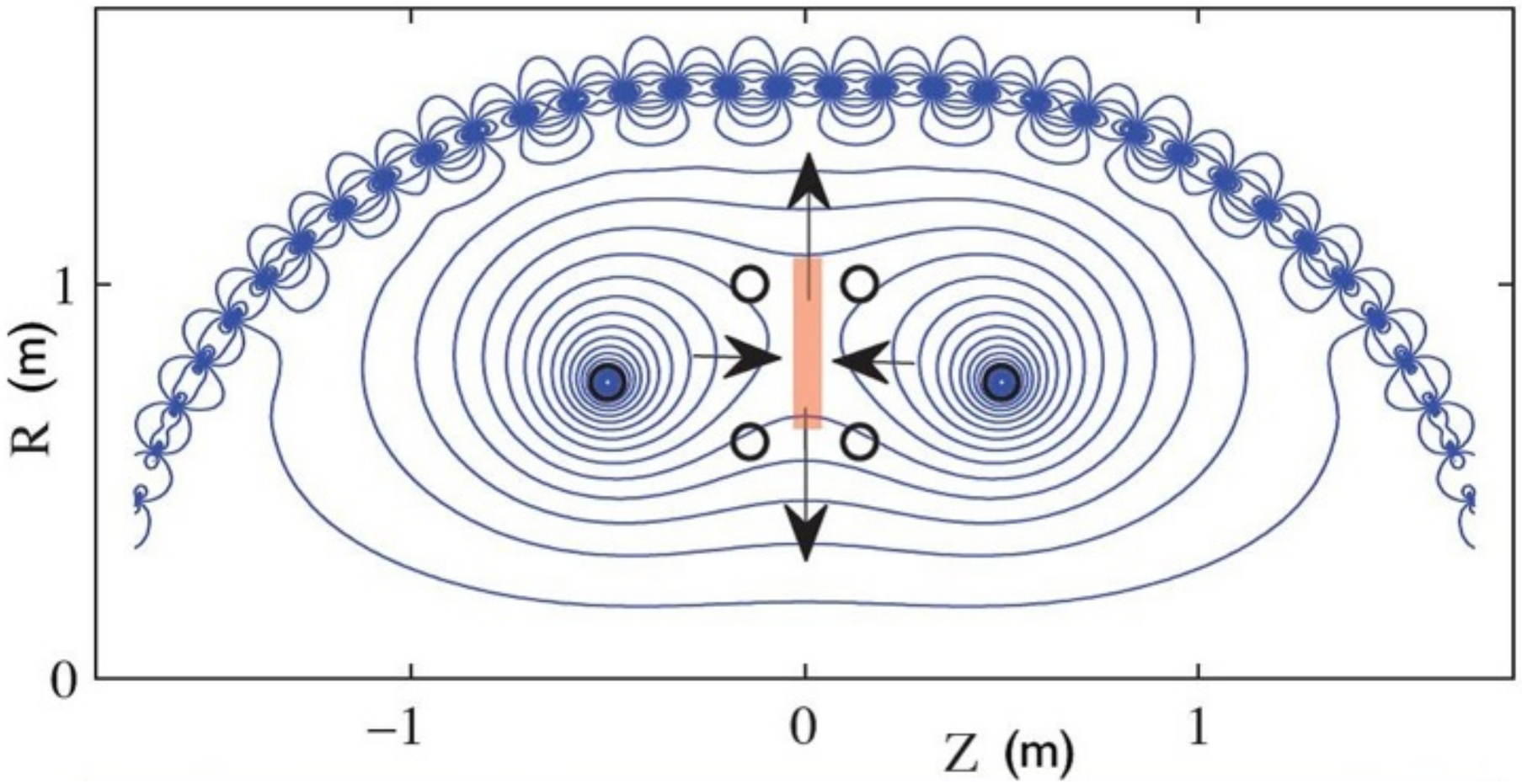

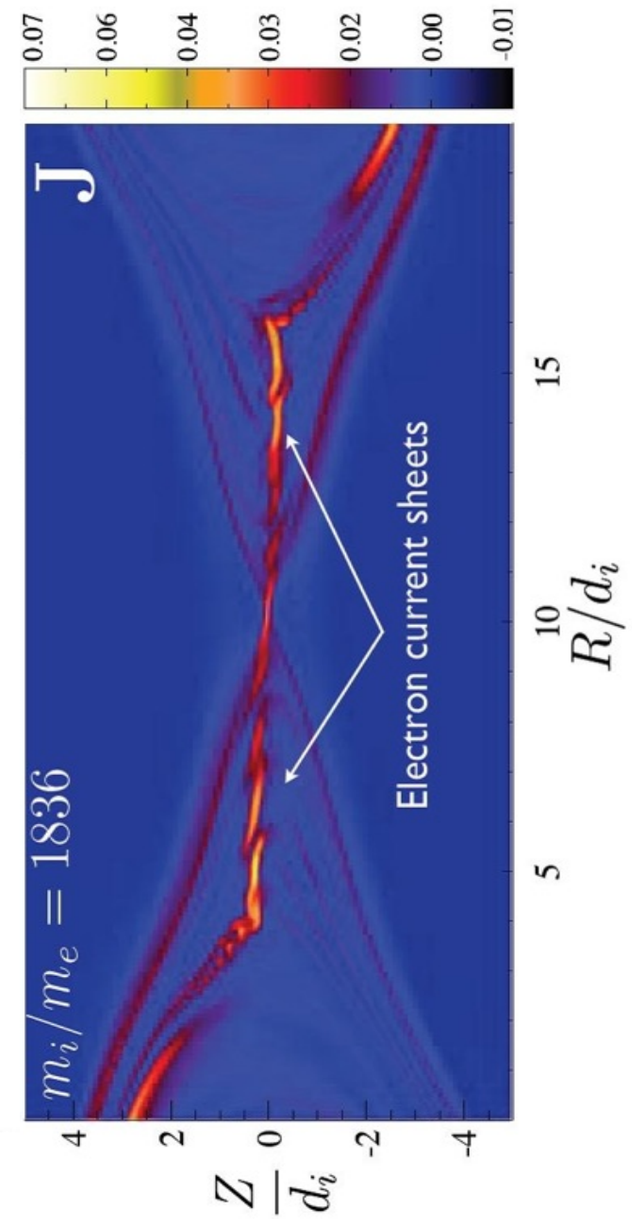

Collisional VPIC simulation

Plasma parameters for Reconnection in TReX

	$n_e/[10^{18}m^{-3}]$	$T_e/[eV]$	$B_r/[T]$	$B_g/[T]$	$L/[m]$
TReX	0.1-10	8 – 40	0.04	0.1	0.8 – 1.6
MRX	1 – 100	5 – 10	0.03	0.1	0.7
Flare	1 – 100	5 – 30	0.15	0.5	1.6
Flare anti par.	1 – 100	5 – 10	0.15	–	1.6

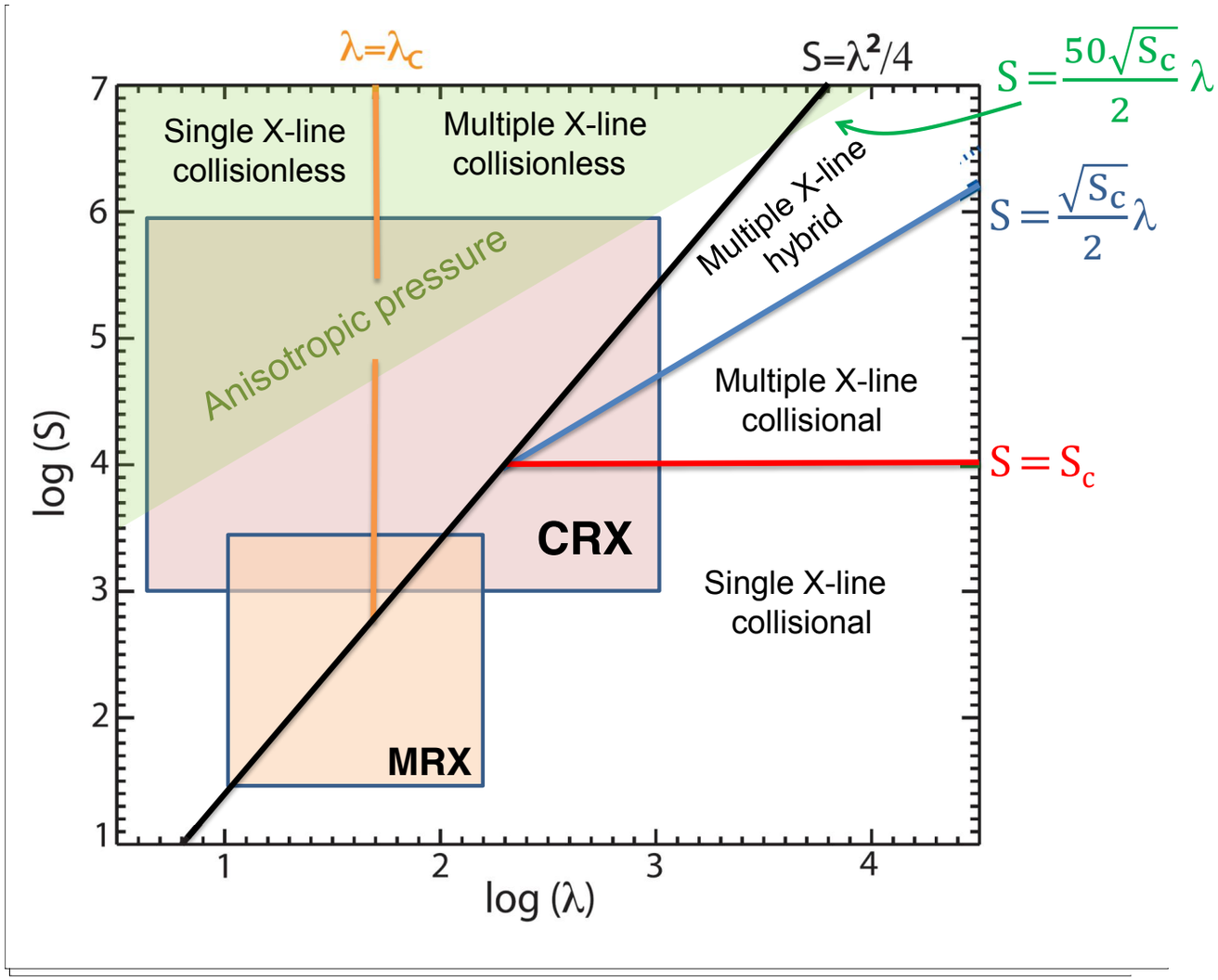

Kinetic simulation: Example of a reconnection current layer driven by pressure anisotropy for $0.1 < B_g/B_r < 0.5$ and $\nu_{ei}/\omega_{ce} < 10^{-4}$.

[Le, et al., PRL 2013]

Out of plane current

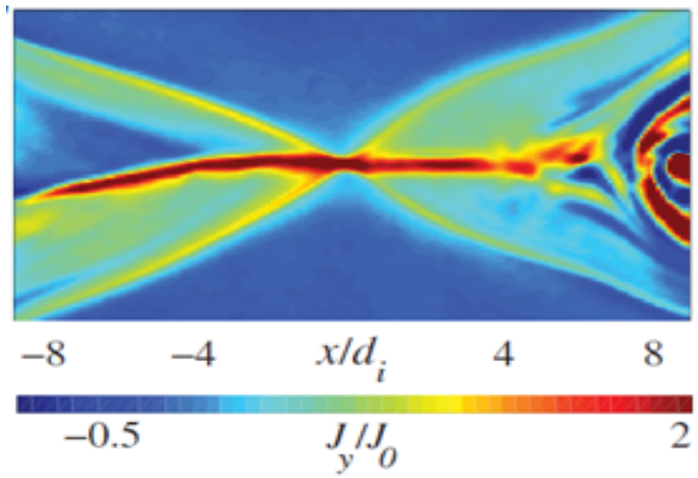

Firehose parameter

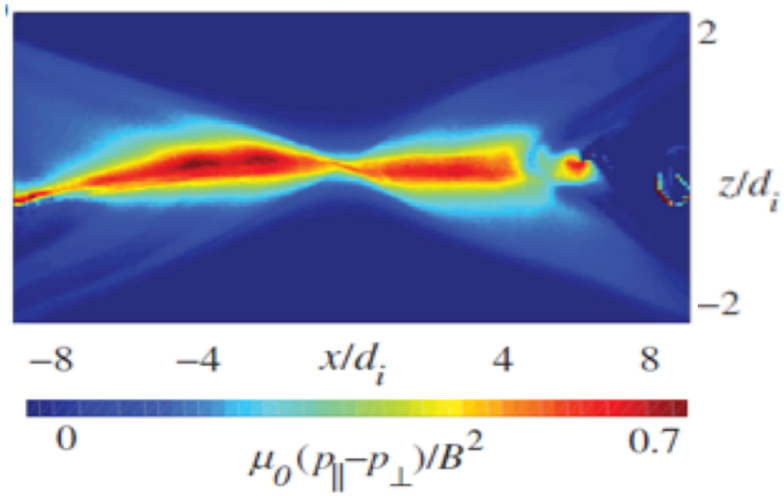

3D null reconnection in TREX

- Configuration using the HH-coils plus internal coil mounted oblique to HH-field

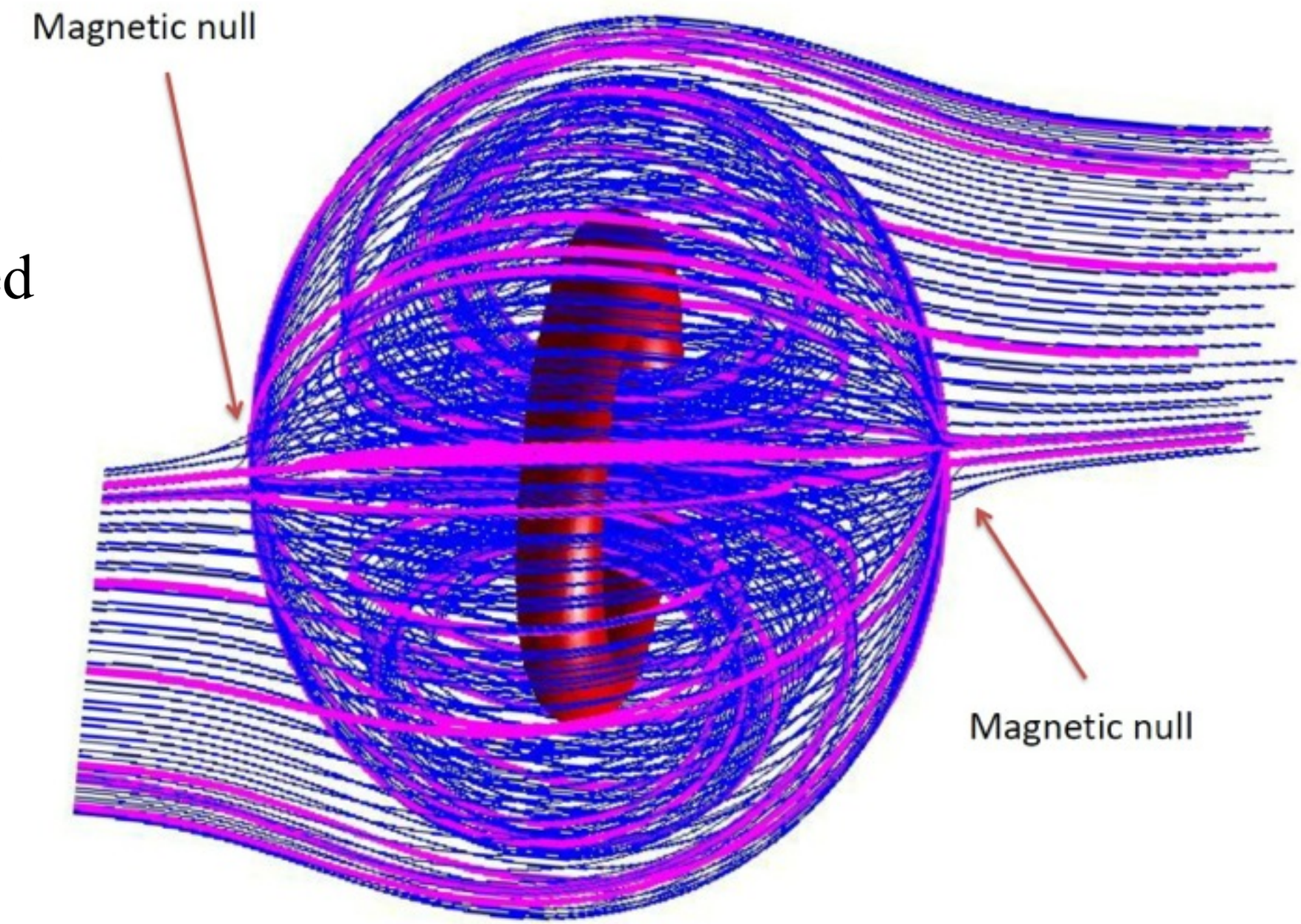

Strong Guide-field Reconnection

- Pulsed operation of magnetic coils
- $B_g = 0.25T$ at 1m
- 3 min between pulses
- Optimize configuration for maximal length of reconnection layer to explore "turbulent reconnection"

Strong guide-field in TREX

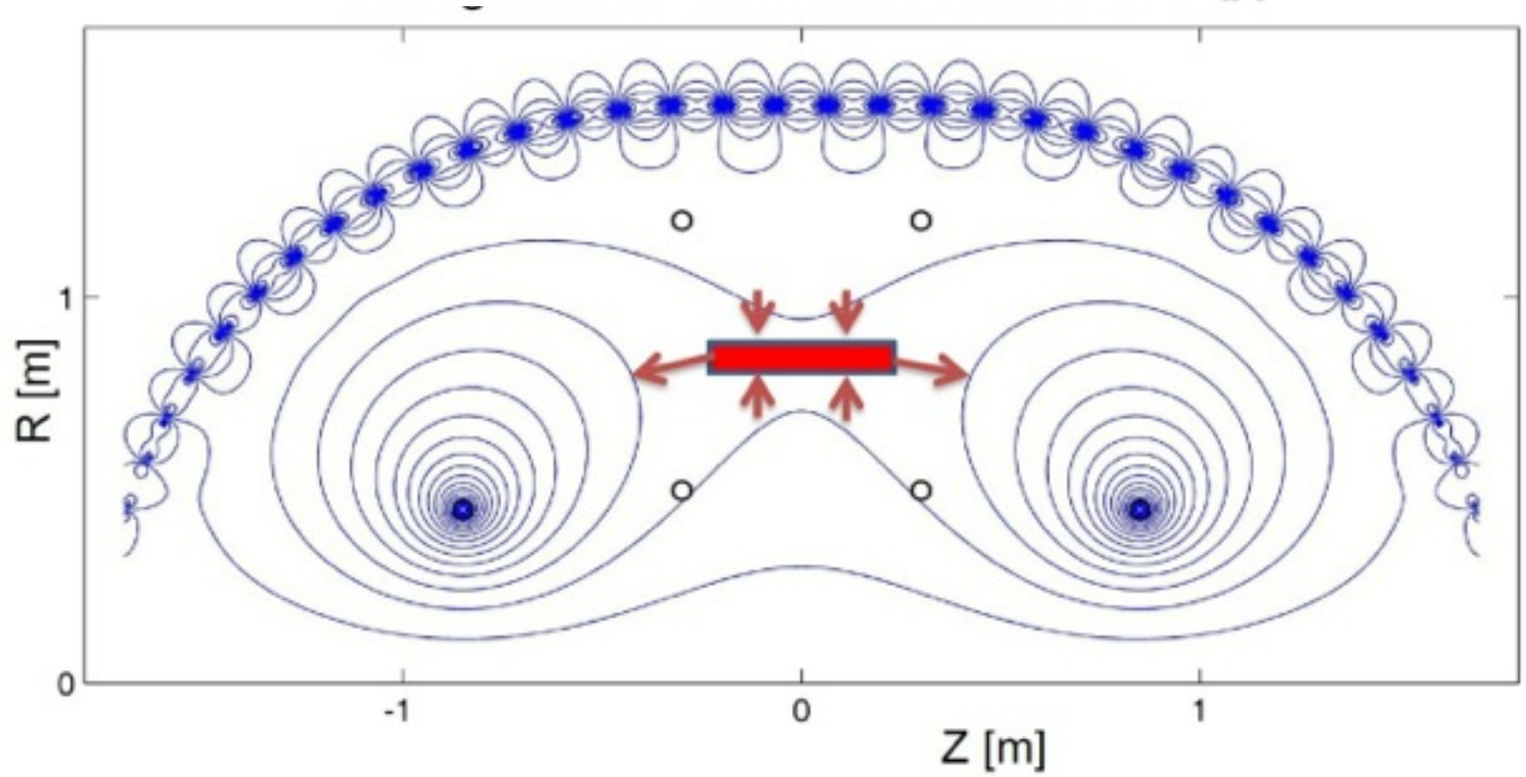

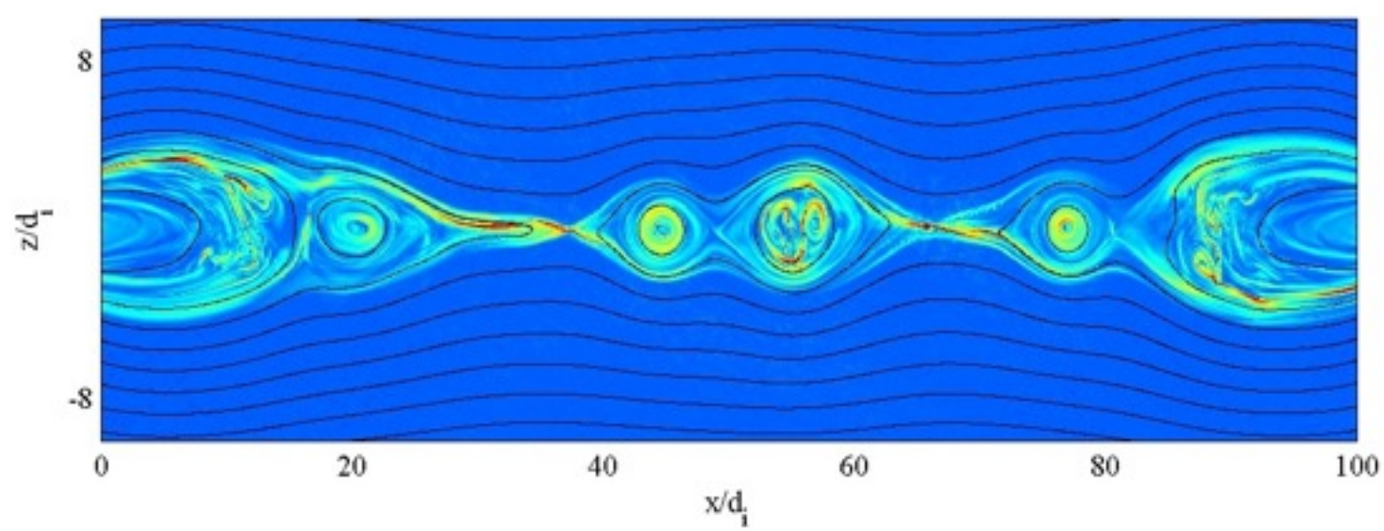

Strong Guide-field Reconnection

- Pulsed operation of magnetic coils
- 3 min between pulses
- $B_g = 0.25T$ at 1m

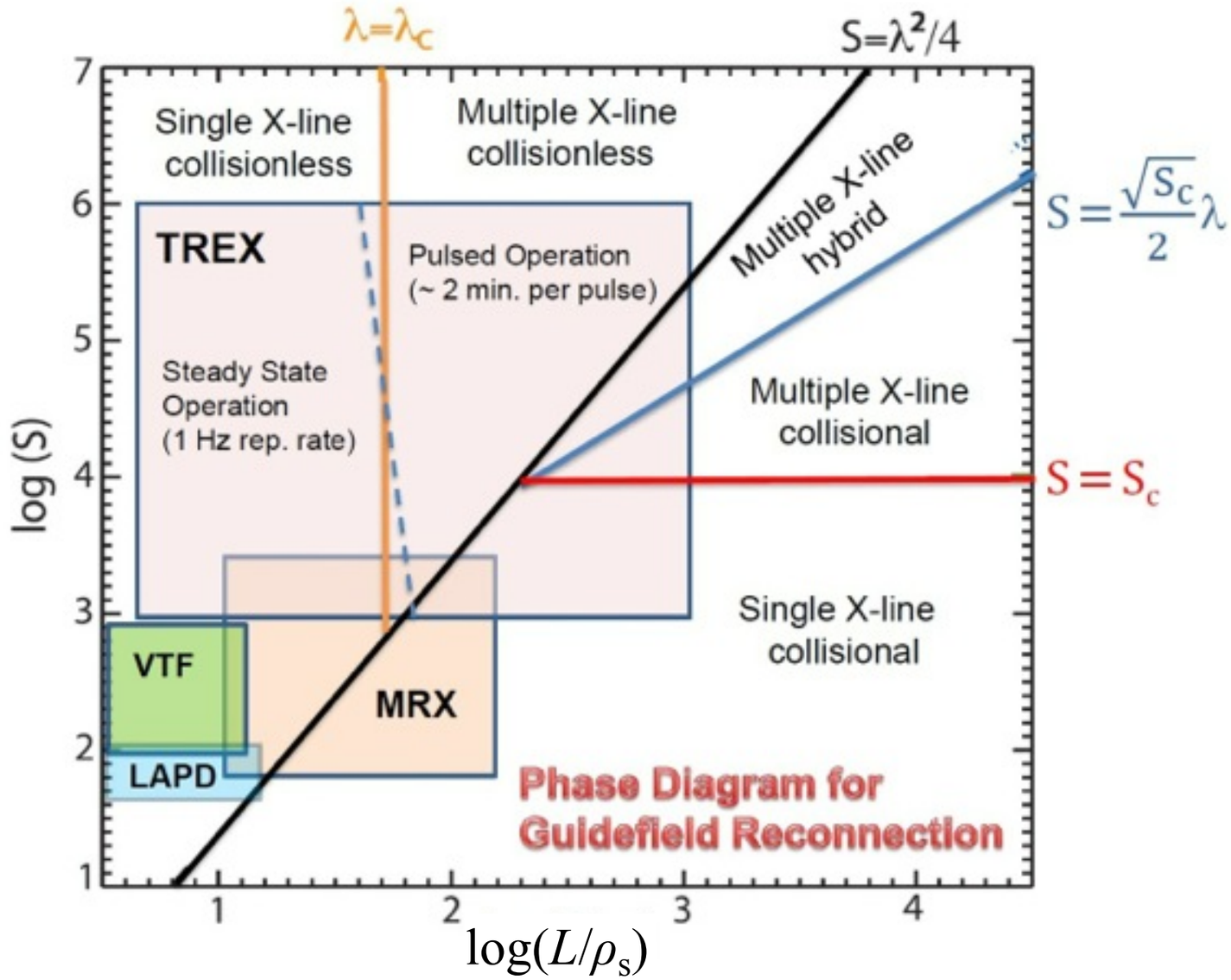

	$n_e/[\mathrm{m}^{-3}]$	$T_e/[\mathrm{eV}]$	$B_r/[\mathrm{T}]$	$B_g/[\mathrm{T}]$	$L/[\mathrm{m}]$
TREX	$10^{17} - 10^{19}$	8 – 40	0 – 0.05	0 – 0.3	0.8 – 2
MRX	$10^{19} - 10^{20}$	5 – 10	0.03	0 – 0.1	0.7
VTF	$10^{17} - 10^{18}$	8 – 30	0.01	0.1	0.3

$\rho_s = (2m_iT_e)^{1/2}/eB$

= "ion sound Larmor Radius"


Thank You

Acknowledgements

Colleagues Weijing Ding, Fatima Ebrahimi, Jan Egedal, Frank Jenko, Mark Nornberg, Klaus Reuter, John Sarff, Erik Spence, Alex Scheckochihin, Fred Skiff, Dennis Whyte, Ellen Zweibel

Engineering John Wallace, Mike Clark

Postdocs Chris Cooper, Kian Rahbarnia, Ivan Khalzov, Ben Brown, Noam Katz

Students Cami Collins, Ken Flanagan, Jon Jara-Almonte, Elliot Kaplan, Jason Milhone, Weifeng Peng, Zane Taylor, David Weisberg

Agencies CMSO, NSF Astro, NSF Physics, DoE